



**BER and SNR PERFORMANCE ANALYSIS OF 2-ASK & 4-ASK  
MODULATED TRUNCATED BESSEL BEAMS ON DIFFERENT  
RECEIVER APERTURES IN FSO COMMUNICATIONS LINKS**

**TEVFİK AĞAR**

**JANUARY 2017**

**BER and SNR PERFORMANCE ANALYSIS OF 2-ASK & 4-ASK  
MODULATED TRUNCATED BESSEL BEAMS ON DIFFERENT  
RECEIVER APERTURES IN FSO OPTIAL COMMUNICATIONS LINKS**

**A THESIS SUBMITTED TO  
THE GRADUATE SCHOOL OF NATURAL AND APPLIED  
SCIENCES OF  
ÇANKAYA UNIVERSITY**

**BY  
TEVFİK AĞAR**

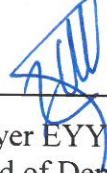
**IN PARTIAL FULFILLMENT OF THE REQUIREMENTS FOR THE  
DEGREE OF  
MASTER OF SCIENCE  
IN  
THE DEPARTMENT OF  
ELECTRONIC AND COMMUNICATION ENGINEERING**

**JANUARY 2017**

**Title of the Thesis: BER and SNR Performance Analysis of 2-ASK & 4-ASK  
Modulated Truncated Bessel Beams on Different Receiver Apertures in FSO  
Communication Links**

Submitted by **Tevfik AĞAR**

Approval of the Graduate School of Natural and Applied Sciences, Çankaya University.

  
\_\_\_\_\_  
Prof. Dr. Halil Tanyer EYYUBOĞLU  
Head of Department

I certify that this thesis satisfies all the requirements as a thesis for the degree of Master of Science.

  
\_\_\_\_\_  
Prof. Dr. Yusuf Ziya UMUL  
Head of Department


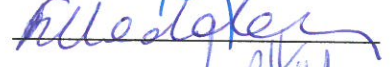
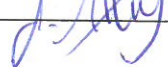
This is to certify that we have read this thesis and that in our opinion it is fully adequate, in scope and quality, as a thesis for the degree of Master of Science.

  
\_\_\_\_\_  
Prof. Dr. Halil Tanyer EYYUBOĞLU  
Supervisor

**Examination Date:** 10.01.2017

**Examining Committee Members**

Prof. Dr. Halil Tanyer EYYUBOĞLU (Çankaya Univ )  
Assoc. Prof. Dr. Firat HARDALAÇ (Gazi Univ.)  
Asst. Prof. Dr. Serap ALTAY ARPALI (Çankaya Univ )

  
\_\_\_\_\_  
  
\_\_\_\_\_  
  
\_\_\_\_\_

## STATEMENT OF NON-PLAGIARISM PAGE

I hereby declare that all information in this document has been obtained and presented in accordance with academic rules and ethical conduct. I also declare that, as required by these rules and conduct, I have fully cited and referenced all material and results that are not original to this work.

Name, Last Name : Tefvik AĖAR

Signature : 

Date : 10.01.2017

## ABSTRACT

### **BER and SNR Performance Analysis of 2-ASK & 4-ASK Modulated Truncated Bessel Beams on Different Receiver Apertures in FSO Communication Links**

AĞAR, Tevfik

M.Sc., Department of Electronic and Communication Engineering

Supervisor: Prof. Dr. Halil Tanyer EYYUBOĞLU

January 2017, 69 pages

In this thesis, varying turbulent atmosphere environment are simulated random phase screen method. 2-ASK & 4-ASK modulated truncated Bessel beam are generated and propagated through turbulent atmosphere utilizing random phase screens. In MATLAB environment error counting method is applied then simulation results are obtained corresponding to BER and SNR. On the other hand, the contributions of enlargement receiver aperture on BER is examined. Also, to comprehend the free space optical (FSO) communication architecture in detail and to support the future experimental studies, FSO communication transmitter and receiver systems are designed.

**Keywords:** Truncated-Bessel Beam, 2-ASK & 4-ASK Modulation, Random Phase Screen, Receiver Aperture Enlargement.

## ÖZ

### **Serbest Uzay Optik Haberleşme Linklerinde, Farklı Alıcı Açıklıkları Üzerinde 2-ASK & 4-ASK Modüle Edilmiş Kesik Bessel Işınının Hatalı Bit ve Sinyal Gürültü Oranlarının Performans Analizleri**

AĞAR, Tevfik

Yüksek Lisans, Elektronik ve Haberleşme Mühendisliği Anabilim Dalı

Tez Yöneticisi: Prof. Dr. Halil Tanyer EYYUBOĞLU

Ocak 2017, 69 sayfa

Bu tezde türbülanslı atmosfer ortamının rastgele faz tabakaları ile simülasyonu yapıldı. 2-ASK & 4-ASK ile modüle edilmiş kesik Bessel ışın huzmesi oluşturulmuş ve oluşturulan ışın huzmesi rastgele faz tabakalarından yararlanılarak türbülanslı atmosfer üzerinden ilerletilmiştir. MATLAB 'da hata sayma metodu uygulandıktan sonra BER ve SNR karşılık gelen simülasyon sonuçları elde edildi. Bir diğer yandan, genişleyen alıcı açıklığının BER üzerindeki katkıları incelendi. Ayrıca, serbest uzay haberleşme sistemi mimarisini daha detaylı kavramak için ve gelecekteki deneysel çalışmalara destek olması açısından FSO haberleşme sistemi vericisi ve alıcısı tasarlandı.

**Anahtar Kelimeler:** Kesik Bessel Işını, 2-ASK & 4-ASK Modülasyon, Rastgele faz tabakaları, Genişleyen Alıcı Açıklığı

## **ACKNOWLEDGEMENTS**

I would like to express my sincere gratitude to Prof. Dr. Halil Tanyer EYYUBOĐLU for his supervision, special guidance, suggestions, and encouragement through the development of this thesis. Additionally, thanks for the support of Mert BAYRAKTAR during the study.

It is a pleasure to express my special thanks to my family for their valuable support.

## TABLE OF CONTENTS

STATEMENT OF NON PLAGIARISM.....	ii
ABSTRACT.....	iii
ÖZ.....	iv
ACKNOWLEDGEMENTS.....	v
TABLE OF CONTENTS.....	vi
LIST OF FIGURES.....	viii
LIST OF ABBREVIATIONS.....	ix
SECTIONS:	Page
<b>1. INTRODUCTION.....</b>	<b>1</b>
<b>1.1. Background of Thesis.....</b>	<b>1</b>
<b>1.2. Scope of Thesis.....</b>	<b>3</b>
<b>1.3. Structure of Thesis.....</b>	<b>5</b>
<b>2. FSO SYSTEM ARCHITECTURE &amp; LABORATORY STUDIES.....</b>	<b>7</b>
<b>2.1. FSO Transmitter System Architecture.....</b>	<b>7</b>
<b>2.1.1 FSO Transmitter System Designed for Laboratory Tests .....</b>	<b>8</b>
<b>2.1.1.1 Clock and Data Generation .....</b>	<b>9</b>
<b>2.1.1.2 Serializer .....</b>	<b>9</b>
<b>2.1.1.3 Laser Driver .....</b>	<b>12</b>
<b>2.1.1.4 Light Source Laser .....</b>	<b>13</b>
<b>2.1.1.5 Transmitter Lens .....</b>	<b>13</b>
<b>2.2. FSO Receiver System Architecture .....</b>	<b>13</b>
<b>2.2.1 FSO Receiver System Designed for Laboratory Tests .....</b>	<b>15</b>
<b>2.2.1.1 Receiver Lens .....</b>	<b>15</b>
<b>2.2.1.2 Avalanche Photodiode (APD) .....</b>	<b>15</b>
<b>2.2.1.3 Trans-impedance Amplifier (TIA) .....</b>	<b>16</b>
<b>2.2.1.4 Limiting Amplifier (LA) .....</b>	<b>16</b>



<b>2.2.1.5</b> Deserializer .....	16
<b>3.</b> ATMOSPHERIC EFFECTS ON FSO LINK.....	18
<b>3.1.</b> Atmospheric Attenuation .....	19
<b>3.1.1</b> Absorption.....	19
<b>3.1.2</b> Scattering .....	20
<b>3.2.</b> Atmospheric Turbulence .....	20
<b>3.2.1</b> Atmospheric Scintillation .....	20
<b>4.</b> RANDOM PHASE SCREEN DERIVATION for TRUNCATED BESSEL BEAM	22
<b>5.</b> ADJUSTING 2-ASK & 4-ASK CONSTELLATION.....	28
<b>6.</b> MATLAB SIMULATION PARAMETER SETTINGS.....	30
<b>7.</b> SIGNAL TO NOISE DERIVATION .....	32
<b>7.1.</b> Shot Noise.....	32
<b>7.2.</b> Thermal Noise.....	33
<b>7.3.</b> Scintillation Noise.....	33
<b>8.</b> EVALUATION OF THE SIMULATION RESULTS.....	36
<b>9.</b> CONCLUSION.....	46
REFERENCES.....	48
APPENDICES.....	56
A. CURRICULUM VITAE.....	56

## LIST OF FIGURES

<b>Figure 1:</b> Transmitter Architecture .....	8
<b>Figure 2:</b> Experimental Implementation of FSO Transmitter System .....	8
<b>Figure 3:</b> Saturn PCB Design PCB Toolkit Software .....	10
<b>Figure 4:</b> The Serializer PCBs Top Layer .....	11
<b>Figure 5:</b> Receiver Architecture .....	14
<b>Figure 6:</b> Experimental Implementation of .....	15
<b>Figure 7:</b> Absorption .....	19
<b>Figure 8:</b> 4-ASK Signal Vector Constellation on the Source Plane.....	29
<b>Figure 9:</b> Decision Boundaries of 4-ASK Symbols on Receiver Side at $C_n^2 = 10^{-13} m^{-2/3}$ .....	29
<b>Figure 10:</b> Optical Link Simulation Model in Turbulent Atmosphere with Random Phase Screen Method .....	31
<b>Figure 11:</b> 2-ASK Modulated Truncated Bessel Beam versus the structure constant for different receiver aperture .....	37
<b>Figure 12:</b> SNR behavior of the 2-ASK Modulated Truncated-Bessel-Beam versus to structure constant for different receiver aperture .....	38
<b>Figure 13:</b> $P_e$ (BER) behavior of the 2-ASK Modulated Truncated-Bessel-Beam versus to structure constant for different receiver aperture.....	39
<b>Figure 14:</b> 2-ASK and 4-ASK Modulated Truncated Bessel Beam Received Powers versus the structure constant with identical receiver aperture .....	40
<b>Figure 15:</b> 2-ASK and 4-ASK Modulated Truncated Bessel Beam SNR against the structure constant with identical receiver aperture.....	41
<b>Figure 16:</b> 2-ASK and 4-ASK Modulated Truncated Bessel Beam BER versus the structure constant with identical receiver aperture.....	42
<b>Figure 17:</b> 2-ASK & 4-ASK Modulated Truncated Bessel Beam versus the structure constant for different receiver aperture .....	43
<b>Figure 18:</b> 2-ASK & 4-ASK Modulated Truncated-Bessel-Beam SNR behaviors versus to structure constant for different receiver aperture.....	44
<b>Figure 19:</b> 2-ASK & 4-ASK Modulated Truncated-Bessel-Beam $P_e$ (BER) behaviors versus to structure constant for different receiver aperture.....	45

## LIST OF ABBREVIATIONS

ASK	Amplitude Shift Keying
APD	Avalanche Photodiode
BER	Bit Error Rate
CDR	Clock and Data Recovery
ECL	Emitter-coupled logic
FSO	Free Space Optics
IM	Intensity Modulation
HSTL	High-speed transceiver logic
LA	Limiting Amplifier
LVC MOS	Low Voltage Complementary Metal Oxide Semiconductor
LVDS	Low-voltage differential signaling
LVTTL	Low-voltage transistor–transistor logic
LVPECL	Low-voltage positive/pseudo emitter-coupled logic
SSTL	Stub Series Terminated Logic
PCB	Printed Circuit Board
Pe	Probability of Error
PLL	Phase-Locked-Loop
PSU	Power-Supply Unit
VCSEL	Vertical Cavity Surface Emitting Laser

## SECTION 1

### INTRODUCTION

#### 1.1 Background of Thesis

Free Space Optical (FSO) communication system is a digital wireless communication that uses optical technology and simply laser beam propagating through the atmosphere from one point to another point to carry the information. The main purpose of the FSO communication system is to transmit the maximum number of bits per second over the maximum possible range with the minimum bit-error-rate (BER) [1]. However, during the laser beam is propagating through the atmosphere, the variations of turbulent parameters induce fluctuation in the scintillation index which leads to atmospheric attenuation or fading of received signal and distortion [2, 3]. These are indicated with communication performance parameters which are SNR and probability of error (Pe) or BER. BER is important performance criteria for an optical communication system so in the literature BER analysis were made corresponding to scintillation index, beam spreading and beam wandering according to wavelength and source size differences in Ref. [4]. Moreover, the strong turbulence effects on BER were demonstrated in Ref. [5].

In this study, optical wave propagating through the turbulent atmosphere, random phase screens are used to simulate modelling of the turbulence. Firstly, random phase screens proposed along the propagation axis in Ref. [6]. Varying number of the phase screens and receiver plane dimension error analysis was made using random phase screen method [7] and the effects of inner scales on scintillation index were examined in Ref. [8]. Relation between theoretical formulations and random phase screen method advanced but applicability of the random phase screen method was considered. To increase the reliability of the random phase screen method and clarify

the concerns in the literature, random phase screen simulation results and experimental measurements were compared in terms of beam divergence, scintillation, coherency, probability density function of irradiance fluctuations then successive numerical agreement was observed among these results [9]. The random phase screen method limitations and dimensions to be determined for an accurate simulation. The constraints of the random phase screen method were studied with respect to beam width, beam wander, coherence diameter, turbulent parameters and propagation range [10]. Nowadays many books and articles include the comprehensive modeling of propagation in turbulent atmosphere utilizing random phase screen method. This method was also implemented on different beam types analyzing intensity profiles and scintillation characteristics under the weak and strong turbulence regimes [11, 12, 13, 14].

In Ref. [15] solving Helmholtz equation Bessel Beam was obtained. Theoretically, Bessel beam is requiring infinite energy that is impossible to realize in practical life. Therefore, Bessel function is multiplied by Gaussian exponential then Bessel-Gauss beam was obtained and propagation of the Bessel-Gauss beam was examined in Ref [16]. Diffraction was arisen acquiring Bessel-Gauss beam so truncation of the beam achieved with the help of apodization apertures [17]. Different modulation techniques such as amplitude shift keying (ASK), phase shift keying (PSK) and frequency shift keying (FSK) investigated under the weak, moderate, strong turbulence conditions in Ref. [18-19]. On the other hand, enlargement of the receiving aperture is studied from the point of scintillation [20, 21, 22].

In this thesis, random phase screen simulation established that is first tested versus to the known analytic results of the literature. After ensuring that our random phase screen setup is running properly, 2-ASK&4-ASK modulated Bessel beam is truncated at the boundaries of a square source plane in MATLAB environment then simulations are implemented under various turbulent atmosphere. Also, effect of the receiver aperture on modulated truncated Bessel beam is analyzed in detail. All simulation results are obtained in terms of BER, received power and signal to noise

ratio (SNR) which are evaluated against communication performance. Besides the simulation studies, FSO communication transmitter and receiver system are designed in the laboratory environment to grasp the optical communication values. It is envisioned that the designs and simulation results of this thesis can be useful for future free space optical communication.

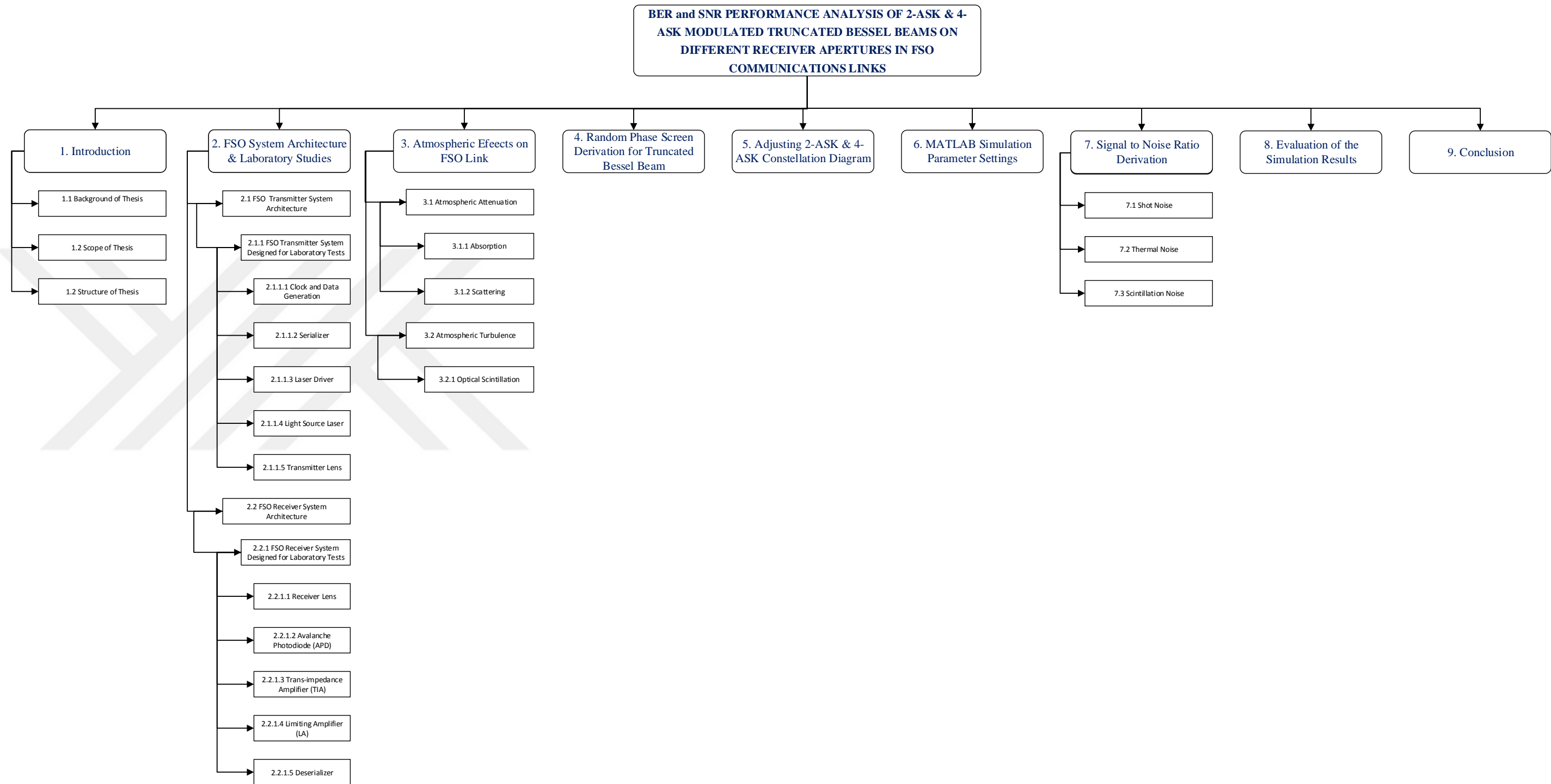
## 1.2 Scope of Thesis

Purpose of this thesis is to investigate the most important performance parameters of an optical communication link like bit-error-rate (BER), Signal to Noise Ratio (SNR), received power on the 2-ASK & 4-ASK modulated truncated Bessel beam and contribution of the receiver aperture during the turbulent atmosphere propagation. In the course of 2-ASK & 4-ASK modulated truncated Bessel beams propagating through turbulent atmosphere, laser beam encounter spatially, temporally refractive index variations of which it is a part of Random Phase Screens. Structure constant is varied between  $C_n^2 = 10^{-15} m^{-2/3}$  which represents the weak turbulence and  $C_n^2 = 10^{-12} m^{-2/3}$  which represents the strong turbulence to simulate turbulent atmosphere effects on truncated Bessel beams. Scintillation index effects are observed on the various receiver aperture and different modulation. Simulation results of Bessel Beam applying 2-ASK and 4-ASK are analyzed considering BER, SNR and received power. During the simulation, source output power is set to 21 mW to enable a meaningful comparison. Theoretically after the symbols randomly generated in the transmitter side applying 2-ASK and 4-ASK modulation, symbols propagated through Random Phase Screens and compared with received symbol to calculate the BER. At the receiver side threshold detection was applied. Stochastically atmospheric fluctuation influences on truncated Bessel beam is examined corresponding to effect of different receiver aperture and 2-ASK & 4-ASK modulation from the viewpoint of optical communication performance parameters.

Also, this thesis emphasis on the methodology to approach free space optical (FSO) communication designs as well as the theoretical working. Therefore, free space optical communication transmitter and receiver system is designed and tested in the laboratory environment to comprehend the FSO communication structure and in the future experimentally will be utilized from these designs.



### 1.3 Structure of Thesis





This thesis comprises from following nine sections:

Section 1 is an introduction that contains history for free space optic communication and scope of this thesis.

In section 2 FSO system architecture is explained in detail. To understand better FSO system architecture and to make a successful experiments in the future, physically high-speed transmitter & receiver circuits are designed and manufactured in laboratory environment as a prototype. The prototype FSO system are tested in the laboratory and performance related observations are explained in section 2.

Section 3 indicates the atmospheric effects over the laser beam.

Random Phase Screen Derivation is demonstrated in section 4 for Truncated Bessel Beam.

2-ASK & 4-ASK constellation diagram is shown in section 5 emphasizing boundary decision region.

Considering rationales, MATLAB simulation settings are explained in section 6.

In section 7 Signal to Noise Ratio derivation is made theoretically.

Section 8 contains evaluation of the simulation results in terms of  $P_e$ , SNR, and received power.

Section 9 has the consequence of thesis.

## SECTION 2

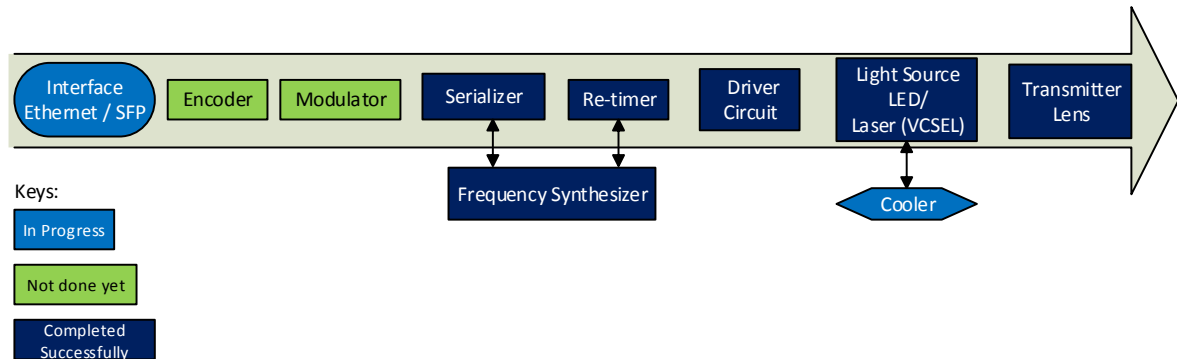
### FSO SYSTEM ARCHITECTURE and LABORATORY STUDIES

In this thesis, Bit Error Rate (BER) concerns such as noise, distortion, interference are regarded on component and (Printed Circuit Board) PCB levels in terms of transmitter and receiver. All design applications and component decisions have been made considering BER factors. In order to reduce the BER in PCB level, Free Space Optic (FSO) system physical application has been implemented and endeavored to improve communication performance.

#### 2.1 FSO Transmitter System Architecture

As it is demonstrated in Figure 1 Transmitter Architecture, FSO Transmitter consists of six main components:

- the original information is reconstructed by encoder from the knowledge of the code [23];
- modulation is mapping information into carrier utilizing the amplitude, phase or frequency [23] and modulator performs modulation to enable transfer of data over a medium [24];
- serializer multiplexes several low speed electrical bit sequence signals to reach a single high speed data stream;
- serial data is marshalling and retiming utilizing phase-locked loop (PLL) [25];
- serialized electrical data stream transmitted the driver which provide high speed current switching operation according to data stream at the input.
- the laser or led converts the electrical data stream to optical data form;
- the transmitter lens system provides collimated beam on the transmitter aperture.

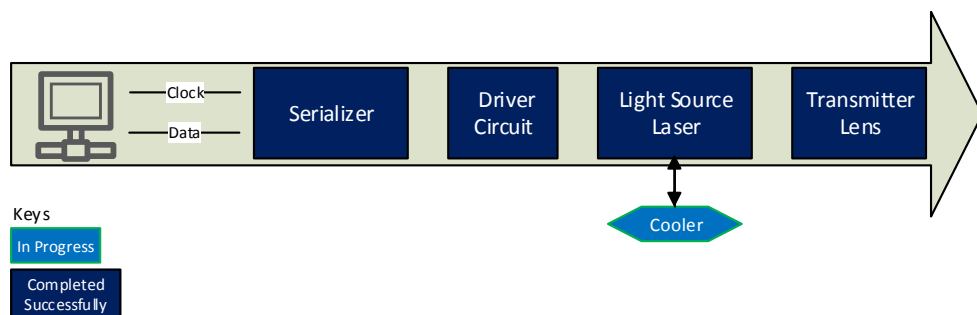


**Figure 1:** Transmitter Architecture

Note: Brief description of the interface has been mentioned in section 2.1.1.1 and 2.1.1.2.

### 2.1.1 FSO Transmitter System Designed for Laboratory Tests

This section gives a short explanation of the experimental transmitter part which is shown in following figure.



**Figure 2:** Experimental Implementation of FSO Transmitter System

### **2.1.1.1 Clock and Data Generation**

IspClock5620A Programmable Clock Generator is programmed by PAC-Designer Software. The designed transmitter is tested with different frequency using the IspClock5620A Programmable Clock Generator. Considering commercial FSO interface applications, Gigabit Ethernet fundamental frequency 125 MHz circuit design is entered into PAC-Designer then the circuit is verified within the PAC-Designer environment. PC parallel port connected to the serial programming interface pins of the IspClock5620A for generating 125 MHz reference clock frequency. In the course of programming the IspClock5620A Programmable Clock Generator, following four critical parameters need to take into consideration which directly influence the design.

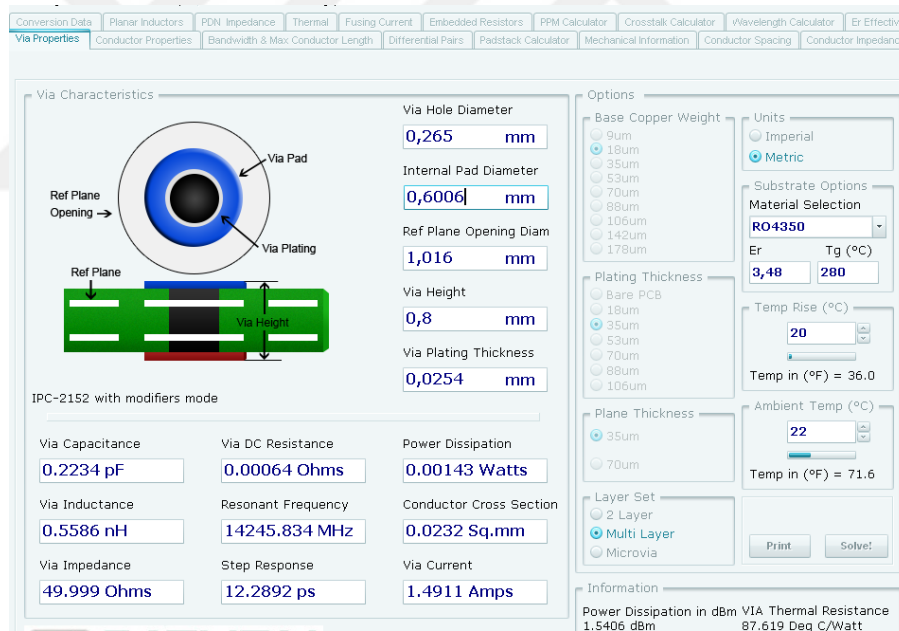
- Operating frequency: 10 MHz to 320 MHz
- Programmable output standards: Low-voltage transistor–transistor logic (LVTTTL), Low Voltage Complementary Metal Oxide Semiconductor (LVCMOS), High-speed transceiver logic (HSTL), Stub Series Terminated Logic (SSTL), Low-Voltage Differential Signaling (LVDS), Low Voltage Complementary Metal Oxide Semiconductor (LVPECL).
- Programmable output impedance: 40  $\Omega$  to 70 $\Omega$
- Programmable slew rate

On the other hand, computer assisted data acquisition device Agilent U2356A digital outputs are configured by Agilent VEE, Agilent T&M Toolkit and MATLAB to set the serializer digital input ports.

### **2.1.1.2 Serializer**

The serializer used for gather several low speed data to reach a sequential high speed data stream which is sent to the laser driver by used serializer. Texas Instrument TLK2211 Gigabit Ethernet Transceiver is selected for FSO communication point-to-

point data physical test. Especially, input voltage type, data speed and input/output impedance are crucial parameters for deciding TLK2211 Gigabit Ethernet transceiver. LVTTTL clock voltage supplied to the TLK2211 by the programmed IspClock5620A. When serializer multiplexes several low speed electrical bit sequence signals to obtain high speed data stream that lead to some communication problems [26]. As the communication of speed increases or frequency of operation increases, to achieve signal integrity problems, serializer clock supplier output impedance and TLK2211 transmission media impedance sets  $50\Omega$  of its corresponding signal source to maximize the power transfer, utilizing Saturn PCB Design PCB Toolkit software which is shown in following figure.



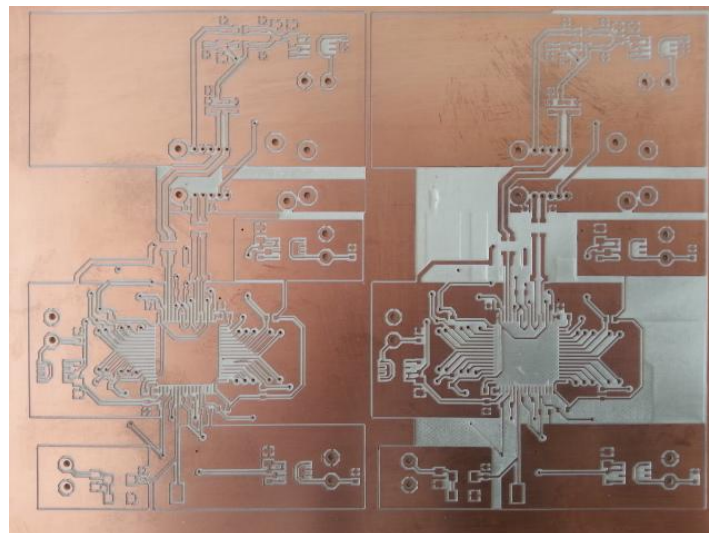
**Figure 3:** Saturn PCB Design PCB Toolkit Software

Actually, vias are minimized as far as possible to avoid signal distortion, when necessary, used Saturn PCB Design PCB Toolkit software.

Especially noise, jitter and interference are major problems for high speed transmitter that have significant effects on communication performance or BER. In this project

hydrocarbon laminates circuit material is decided instead of standard epoxy/glass FR-4 printed-circuit board (PCB) for high speed transmitter to avoid noise, jitter and interference. Choosing high frequency circuit material for a high speed application PCB is generally a tradeoff in terms of some particular parameters. In this thesis, Rogers Corporation RO4350B hydrocarbon ceramic laminate is chosen for controlled impedance transmission lines, minimum signal loss and thermal stress resistance. Particularly, thermal stress resistance is the greatest concern for me during PCB assembly from solder rework since PCB components are assembled by my hands using reflow soldering method.

On the other hand, PCB drilling process is concerned with creating clean holes [27], matching via impedance, minimizing signal noise and reflection, for high speed connections from one conductive layer to another. Regarding these parameters, two diver serializer PCB (shown in below picture) which are subjected to different PCB drilling process using contour routing and rubout method was studied. Rubouting irrelevant cells should minimize noise and to prevent redundant radiation and reflection.



**Figure 4:** The Serializer PCBs Top Layer

To be able to achieve high performance communication the serializer has been designed by taking PCB high frequency material and PCB engraving process into consideration.

Mainly, the TLK2211 performs the data serialization (during send operation), deserialization (during receive operation) for physical layer interface operations. The 10-bit interface (TBI) mode is selected in accordance with IEEE 802.3 Gigabit Ethernet. The Physical Coding Sublayer (PCS) maps Gigabit Media Independent Interface (GMII) into ten-bit code groups and vice versa (for deserializing), using an 8b/10b block coding scheme signals [28] then 8b/10b parallel encoded data bytes are sequentially transmitted from bit 0 to bit 9 on the rising edge of the clock.

Consequently, serializer PCB design has been optimized according the operating frequency as much as possible. Clock buffer is used to prevent clock glitch and to minimize reference clock noise. Stable and low noise voltage regulators are preferred for high performance application. Concordantly, the voltage regulator ground planes are divided into varied groups to isolate parasitic noise which prevents interference of the different noise level.

### **2.1.1.3 Laser Driver**

The LTC5100 VCSEL Driver is selected for use in the experimental implementation of transmitter part that is driven with different modulation currents from 1mA to 12mA. Mainly VCSEL Driver process high speed current switch which is directly affected and controlled by modulated data stream at the input. The selected VCSEL driver behaves as a constant current source rather than voltage power supply unit therefore, voltage fluctuations can be caused dramatic changes on the modulation current and laser output. LTC5100 modulation current and bias current are configured by EEPROM 24LC00 [1]. VCSEL control parameters were simulated by LTC5100 Evaluation Software and programmed by PikProg2. Depend on needs and

requirements, the device parameters are adjusted utilizing non-volatile memory so LTC5100 produces laser currents in response to digitally programmed commands

#### **2.1.1.4 Light Source Laser**

HFE4093-342 VCSEL laser is used for laboratory test. Considering modulation current and communication data speed HFE4093-342 VCSEL is chosen from Honeywell optical products. This VCSEL operate with drive currents between 3-15mA correspondingly LTC5100 modulation current. This high-performance device is designed for high-speed data communication which provides operation from DC to 2.5 Gbps that means experimental test requirements corresponded using HFE4093-342 VCSEL.

#### **2.1.1.5 Transmitter Lens**

Practically laser emits a light, but the emitted light prone to diverge from propagation axis therefore, collimator is used for concentrating and aligning divergent lights in a specific direction. Collimated rays propagate from spatial cross section to constitute a beam form. Generally, in the laboratory environment beam spot size is small because of limited laser propagation range so enlargement of the beam cross section is utilized from beam expander. In this study, collimator and beam expander have been selected from Thorlabs optical device Manufacturer Company with necessary alignment tools.

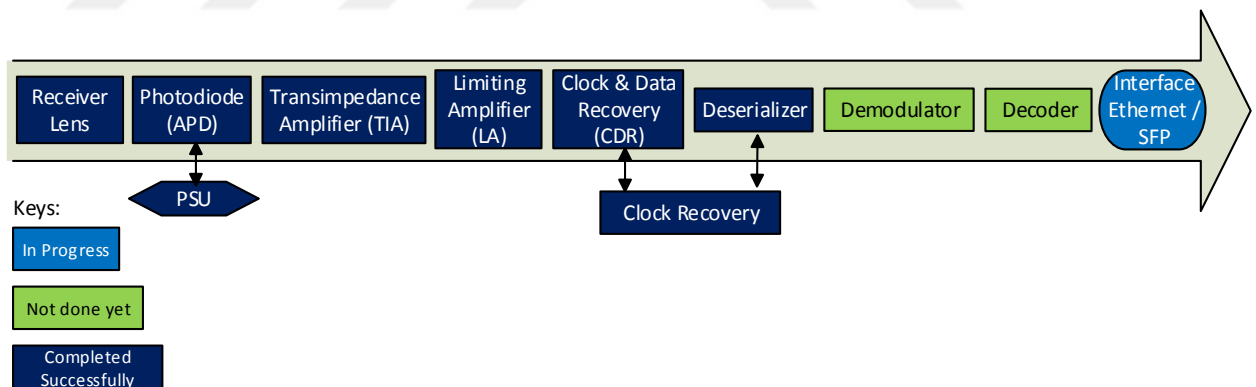
### **2.2 FSO Receiver System Architecture**

Receiver Architecture consists of eight main components which are illustrated figure 5:

- the receiver lens collects and focuses coming photons over the photodiode active area;



- the purpose of photodiode is to convert optical data to electrical data form utilizing photons;
- the trans-impedance amplifier converts the small photocurrent (which is coming from photodiode) into reasonable output voltage to connect limiting amplifier;
- the limiting amplifier has a high gain to provide maximum voltage amplification;
- the aim of the clock & data recovery circuit is to separate clock and data removing noise [25, 30];
- single high speed long data streams are divided and arranged by deserializer;
- the demodulator provides to reverse process of modulation which is removing the carrier signal to obtain the original signal waveform back [23];
- the decoder maps the encoded data into the transmitted user data using channel output information [23].

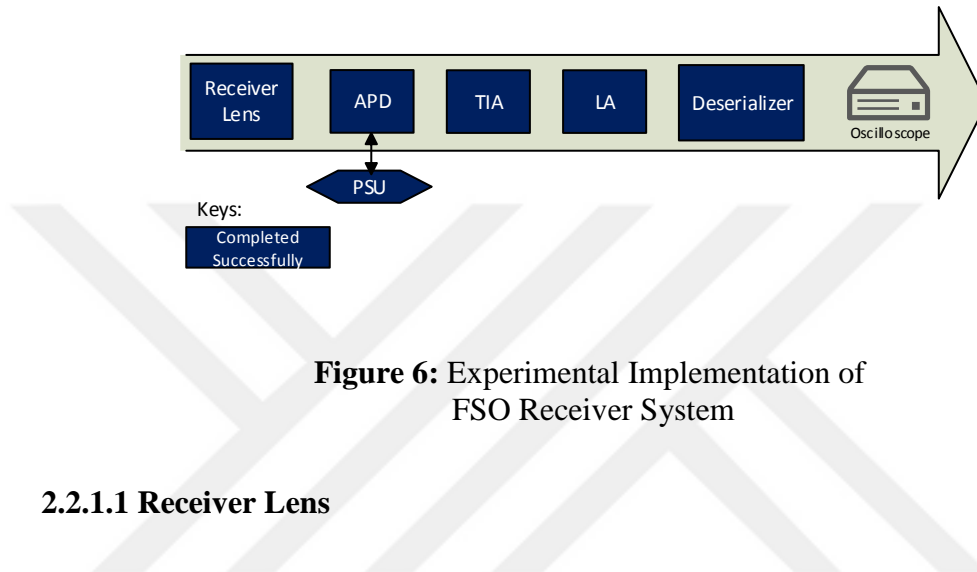


**Figure 5:** Receiver Architecture

Assuming the line-of-sight laser communication is established and concentrated beam is received from transmitter properly. In this study, laser communication receiver system is terminated with oscilloscope instead of demodulator and decoder circuits which is demonstrated on the section 2.2.1 FSO Receiver System Designed for Laboratory Tests.

## 2.2.1 FSO Receiver System Designed for Laboratory Tests

Experimental implementation of receiver part is demonstrated following figure 6.



**Figure 6:** Experimental Implementation of FSO Receiver System

### 2.2.1.1 Receiver Lens

Generally, the most important optical component of FSO communication is receiver lens system. In the transmitter side generated a beam that needs to focus on photodiode active area reducing the undesirable background light in the receiver side perfectly. Bearing in mind that undesirable noises, anti-reflective coated achromatic mounted lens is chosen from Thorlabs. Firstly, all optical studies have been simulated in the ZEMAX, afterward the ensuring that optical design is working properly, optical components have been purchased.

### 2.2.1.2 Photodiode (APD)

Photodiode is one of the fundamental part in optical communication receiver system which has a big effect on the receiver performance. Deciding photo-detector following parameters should be bear in mind:

Operation wavelength, APD gain, dark current, rise-time and bandwidth. AD230-8 Avalanche Photodiode is selected for this laboratory application. Power Supply Unit (PSU) is used for arranging gain factor.

#### **2.2.1.3 Trans-impedance Amplifier (TIA)**

Trans-impedance amplifier (TIA) is used to convert small photodiode currents into usable voltage signals. MAX3744 is selected for this receiver application. Selecting TIA essential parameters are identified with the help of comprehensive research. Modeling photodiode as a current source, we need to consider about impedance, capacitance and desired bandwidth. Emphasizing stability of the usable voltage signal gain, capacitance values need to be considered to avoid oscillation [31, 32].

#### **2.2.1.4 Limiting Amplifier (LA)**

TIA output has a small signal which is need to reach detectable level so MAX3748 Limiting Amplifier (LA) is chosen for voltage amplification that is suggested by MAXIM. LA is located in between TIA and deserializer which comprise different medium therefore LA medium ground plane need to be separated from deserializer and connections should be provided AC-coupling. On the other hand, between TIA and LA DC-coupling connections are need to be checked in terms of DC voltage level (offset) to prevent LA saturation [33]. After the signal has been amplified to detectable logic levels, signal is sent to the deserializer.

#### **2.2.1.5 Deserializer**

As explained in section 2.1.1.2 Serializer, the serializer and deserializer need to be identical therefore TLK2211 Gigabit Ethernet transceiver is chosen for receiver deserializing operation. When high speed serial data is demultiplexed by deserializer

to multiple low speed parallel data channels, clock and data recovery (CDR) and deserializer need to be bear from same precise clock source to avoid phase and frequency problems [25].



## SECTION 3

### ATMOSPHERIC EFFECTS ON FSO LINK

In fact, free space optical communication performance depends not only on its intrinsic design features but also affected by atmospheric varying parameters. Laser beam propagation through the atmosphere is a phenomenon for FSO communication system. When laser beam is propagating through the atmosphere, beam encounters with varying parameters such as chemical composition, temperature, humidity, pressure and air movement over time and the path of the propagating beam [34]. Continuously changing atmospheric parameters causes dynamic, unguided and random environment. Due to varying parameters, atmosphere has an adverse effect on the propagating laser beam. Thus it is useful to know how FSO systems are affected by different weather and climatic conditions. In this thesis, fluctuation atmosphere effects are researched into two groups which are described in the below:

1. Atmospheric Attenuation
  - Absorption
  - Scattering
2. Atmospheric Turbulence
  - Optical Scintillations

Assuming line-of-sight laser communication has been established between transmitter and receiver under the weak -turbulence conditions. Generally, during laser propagation the classical approach in a turbulent medium examined with the first-order approximation of the Rytov method [35, 36]. Rytov-method higher-order terms are used for to investigate atmospheric large-scale scattering components (strong turbulent medium) and geometrical effects which includes beam wandering, beam spreading beam jittering, wave-front distortions, angle-of-arrival fluctuations [37]. First-order Rytov approximation is applicable for this thesis because of weak-turbulence atmospheric conditions. Furthermore, Rytov method is also known that

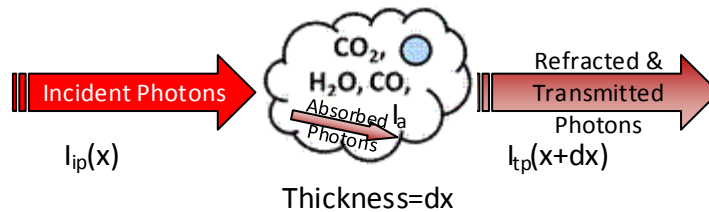
method of smooth perturbations in literature and the limits of the applicability for the Rytov method demonstrated in the Pisareva's article in terms of received signal intensity & phase [38].

### 3.1 Atmospheric Attenuation

Absorption and scattering deterministic main parameters can be simulated by utilizing Lowtran, Fascode, Modtran, Hitran, and Lnpwin software. Modtran is a fairly well known atmospheric radiative transfer model software since its accuracy is validated by US Air Force Research Laboratory.

#### 3.1.1 Absorption

When beam is propagating in the atmosphere, photons come across with water vapor, carbon dioxide, nitrous oxide, carbon monoxide, ozone, nitrogen, oxygen and aerosols [39] in terrestrial atmosphere, results from the interaction between the different mediums, which leads to loss of photon energy. During the light beam traveling through an absorbing medium of thickness  $dx$  which is shown in figure 7, intensity of the photons after thickness is calculated with help of formula 3.1 [39].



**Figure 7:** Absorption

$$I_{tp}(\lambda, x+dx) = I_{ip}(\lambda, x) - dI_a(\lambda, x) \quad (3.1)$$

Incident photons are propagating with wavelength  $\lambda$ . When they encounter with absorbent medium, they are losing energy throughout the absorbent medium which is represented with following formula:

$$dI_a(\lambda, x) = a(\lambda, x)I_{ip}(\lambda, x) \quad (3.2)$$

$a(\lambda, x)$  shows the absorbing medium properties.

### 3.1.2 Scattering

During the laser beam propagation of the atmosphere, scattering arises from the interaction between photons and molecules that causes angular redistribution upon the incident wave with or without modification of the wavelength. If incident waves scatter from medium with the same wavelength, Rayleigh (molecular) Scattering and Mie (aerosol) Scattering can be mentioned, otherwise Raman Scattering is applicable. When we look at the literature of atmosphere physics, Raman scattering is stated inelastic form of scattering because of wavelength change involvement [40]. Considering the selected operating laser wavelength and particle size, Mie scattering is applicable for this thesis [41]. In this thesis scattering evaluated with following formula [42]:

$$\rho_\lambda = NC\pi r_p^2 \quad (3.3)$$

where N gives the number of particles,  $r_p$  indicates the radius of the particle and C is selected 2 since operating wavelength is close to particle size.

## 3.2 Atmospheric Turbulence

### 3.2.1 Optical Scintillation

The source beam propagating through the atmosphere, small temperature and refraction index variations cause intensity fluctuations on the receiver. These type of turbulence effects are theoretically modeled with Rytov approximation which is

applicable for this thesis and logarithmic amplitude variance has been calculated with following formula [43].

$$\sigma_x = 0.5631k^{7/6} \int_0^z C_n^2(L)(L/z)^{5/6}(z-L)^{5/6} dL \quad \text{unitless (3.4)}$$

where  $C_n^2$  is the index of refraction structure parameter,  $k = 2\pi/\lambda$  optical wave number,  $\lambda$  is wavelength,  $L$ (m) is instantaneous distance, and  $z$  (m) is the propagation path length between transmitter and receiver .





## SECTION 4

### RANDOM PHASE SCREEN DERIVATION for TRUNCATED BESSEL BEAM

When the FSO communication literature was reviewed, scintillation investigation and evaluation on various beams were utilized random phase screen method [44-47]. The propagation of the source beam through the atmosphere that spatially and temporally refractive index variations and the consequent turbulence effects are modeled and analyzed by random phase screen method. This method is very close to physical reality and mainly provide advantages that we can generate different source beams avoiding difficult analytic deviations, easily create various atmospheric propagation conditions and examine the source beam, the received beam with independent propagation conditions. Considering these advantages, we have studied with random phase screen method and analytical expression is written benefitting from the lecture notes on Random Phase Screen by Eyyuboğlu, H.T [43, 48]. On the receiver plane intensity at the end of communication link can be expressed with following double integral formula utilizing Huygens-Fresnel Principle:

$$\begin{aligned}
 u_e \mathbf{e}, z &= \frac{-jk \exp jkz}{2\pi z} \int_{-\infty}^{\infty} \int_{-\infty}^{\infty} d^2 \mathbf{u}_i \mathbf{i} \exp \left[ \frac{jk}{2z} \mathbf{e} - \mathbf{i}^2 \right] \quad \text{with } \mathbf{i} = i_x, i_y, \quad \mathbf{e} = e_x, e_y \\
 u_e e_x, e_y, z &= \frac{-jk \exp jkz}{2\pi z} \int_{-\infty}^{\infty} \int_{-\infty}^{\infty} di_x di_y u_i i_x, i_y \exp \left\{ \frac{jk}{2z} \left[ e_x - i_x^2 + e_y - i_y^2 \right] \right\} \\
 &= \frac{-jk \exp jkz}{2\pi z} \int_{-\infty}^{\infty} \int_{-\infty}^{\infty} di_x di_y u_i i_x, i_y \exp \left\{ \frac{jk}{2z} \left[ -2i_x e_x - 2i_y e_y + i_x^2 + i_y^2 + e_x^2 + e_y^2 \right] \right\} \quad (4.1)
 \end{aligned}$$

where  $z$  refers to the propagation distance between transmitter and receiver,  $i_x, i_y$  indicate incident source plane coordinates and  $e_x, e_y$  show end receiver plane

coordinates at the end,  $u_e e_x, e_y, z$  demonstrates received field which was passed through turbulent atmosphere. Considering  $i_x, i_y$  parameters, above formulation integrated inner exponential term in can be demonstrated as below:

$$u_e e_x, e_y, z = \frac{-jk \exp jkz}{2\pi z} \exp\left[\frac{jk}{2z} e_x^2 + e_y^2\right] \int_{-\infty}^{\infty} \int_{-\infty}^{\infty} di_x di_y u_i i_x, i_y \exp\left[\frac{jk}{2z} i_x^2 + i_y^2\right] \exp\left[-\frac{jk}{z} i_x e_x + i_y e_y\right] \quad (4.2)$$

Fourier transform is calculated to change the planes from transmitter to receiver planes as shown in the following expression:

$$u_e e_x, e_y, z = \frac{-jk \exp jkz}{2\pi z} \exp\left[\frac{jk}{2z} e_x^2 + e_y^2\right] \mathbf{F}^{-1} \left\{ \mathbf{F} \left[ u_i i_x, i_y \right] \mathbf{F} \left\{ \exp\left[\frac{jk}{2z} i_x^2 + i_y^2\right] \right\} \right\} \quad (4.3)$$

$\mathbf{F}$  indicates the Fourier transform operation. Additionally, Eq.4.3 is an extraordinary equation, because it contains both one Fourier Transform, one inverse Fourier Transform, however it helps with fixed scaling between the transmitter and receiver planes. Hence, Eq.4.1 can be simply written as

$$u_e e_x, e_y, z = \int_{-\infty}^{\infty} \int_{-\infty}^{\infty} di_x di_y u_i i_x, i_y k e_x - i_x, e_y - i_y \quad (4.4)$$

When as compared to Eq.4.1 and Eq.4.4,  $t$  which is the impulse response is defined and can be written in both forms as

$$t x, y = \frac{-jk \exp jkz}{2\pi z} \exp\left[\frac{jk}{2z} x^2 + y^2\right],$$

$$t e_x - i_x, e_y - i_y = \frac{-jk \exp jkz}{2\pi z} \exp\left\{\frac{jk}{2z} \left[ e_x - i_x^2 + e_y - i_y^2 \right]\right\} \quad (4.5)$$

Hence Eq.4.4 simplified to the basic form of Eq.4.6 as stated below

$$u_e e_x, e_y, z = u_i i_x, i_y \otimes t e_x, e_y \quad (4.6)$$

where  $\otimes$  operation performs the convolution operation between  $u_i i_x, i_y$  and  $t e_x, e_y$ . Using Eq.4.6, it is difficult to reach the simulation result. Because of that reason, Eq.4.6 should be analyzed in detail as

$$u_e e_x, e_y, z = \mathbf{F}^{-1} \mathbf{F}[u_i i_x, i_y] \mathbf{F}[t e_x, e_y] = \mathbf{F}^{-1} \mathbf{F}[u_i i_x, i_y] T f_x, f_y \quad (4.7)$$

Next step is to calculate the Fourier Transform of  $t x, y$  impulse response [5], and then Eq.4.7 turns into

$$\begin{aligned} \mathbf{F}[t x, y] &= T f_x, f_y = \exp jkz \exp \left[ -\frac{2j\pi^2 z}{k} f_x^2 + f_y^2 \right] \\ &= \exp jkz \exp \left[ -j\pi\lambda z f_x^2 + f_y^2 \right] \end{aligned} \quad (4.8)$$

However, it is said in [49], source and transmitter plane coordinates seem similar to each other. To clarify the difference between them, relationship between these parameters are written as  $\mathbf{e} = a_f \mathbf{i}$  defining a scaling term as.

$$\mathbf{e} - \mathbf{i}^2 = a_f \left( \frac{\mathbf{e}}{a_f} - \mathbf{i} \right)^2 - \left( \frac{1-a_f}{a_f} \right) \mathbf{e}^2 + 1-a_f \mathbf{i}^2 \quad (4.9)$$

Then Eq.4.9 is substituted into Eq.4.1, and it becomes

$$u_e \mathbf{e}, z = \frac{-jk \exp jkz}{2\pi z} \exp \left[ \frac{jk}{2z} \left( \frac{a_f - 1}{a_f} \right) \mathbf{e}^2 \right] \int_{-\infty}^{\infty} \int_{-\infty}^{\infty} d^2 \mathbf{i} u_i \mathbf{i} \exp \left[ \frac{jk}{2z} a_f \left( \frac{\mathbf{e}}{a_f} - \mathbf{i} \right)^2 \right] \exp \left[ \frac{jk}{2a} 1-a_f \mathbf{i}^2 \right] \quad (4.10)$$

$u_{i1} \mathbf{i}$  is introduced as below

$$u_{i1} \mathbf{i} = \frac{1}{a_f} u_i \mathbf{i} \exp \left[ \frac{jk}{2z} 1-a_f \mathbf{i}^2 \right] \quad (4.11)$$

Then, Eq.4.10 is rewritten as

$$u_e \mathbf{e}, z = \frac{-jk \exp jkz}{2\pi z} \exp \left[ \frac{jk}{2z} \left( \frac{a_f - 1}{a_f} \right) \mathbf{e}^2 \right] \int_{-\infty}^{\infty} \int_{-\infty}^{\infty} d^2 \mathbf{i} a u_{i1} \mathbf{i} \exp \left[ \frac{jk}{2z} a_f \left( \frac{\mathbf{e}}{a_f} - \mathbf{i} \right)^2 \right] \quad (4.12)$$

Eq.4.12 re-organized utilizing the scaling  $\mathbf{e}_1 = \mathbf{e}/a_f$ ,  $z_1 = z/a_f$

$$u_e \mathbf{e}, z = \frac{-jk \exp jkz}{2\pi z} \exp \left[ \frac{jk}{2z} \left( \frac{a_f - 1}{a_f} \right) \mathbf{e}^2 \right] \int_{-\infty}^{\infty} \int_{-\infty}^{\infty} d^2 \mathbf{i} a u_{i1} \mathbf{i} \exp \left[ \frac{jk}{2z_1} \mathbf{e}_1 - \mathbf{i}^2 \right] \quad (4.13)$$

Here, it is clear that scaling must be applied, since integral boundaries are infinite. In addition to this information, in Eq.4.13. there is a convolution relationship but it is difficult so extract some of the term out of the integral. Hence, this equation re-organized using impulse response as

$$u_e \mathbf{e}, z = \exp jkz \exp \left[ \frac{jk}{2z} \left( \frac{a_f - 1}{a_f} \right) \mathbf{e}^2 \right] \int_{-\infty}^{\infty} \int_{-\infty}^{\infty} d^2 \mathbf{i} a u_{i1} \mathbf{i} t \mathbf{e}_1 - \mathbf{i} \quad (4.14)$$

where

$$t \mathbf{e}_1 - \mathbf{i} = \frac{-jk}{2\pi z} \exp \left[ \frac{jk}{2z_1} \mathbf{e}_1 - \mathbf{i}^2 \right] \quad (4.15)$$

Eq.4.15 turn into below Eq.4.16 after calculating the Fourier transform

$$T \mathbf{f} = \mathbf{F}[t \mathbf{e}_1 - \mathbf{i}] = \exp -j\pi\lambda z_1 \mathbf{f}^2 = \exp \left( -j\pi\lambda \frac{z}{m_f} \mathbf{f}^2 \right) = \exp \left( -\frac{2j\pi^2 z}{m_f k} \mathbf{f}^2 \right) \quad (4.16)$$

Consequently, Eq.4.14 is expanded in the form of

$$\begin{aligned} u_e \mathbf{e}, z &= \exp jkz \exp \left[ \frac{jk}{2z} \left( \frac{a_f - 1}{a_f} \right) \mathbf{e}^2 \right] u_{i1} \mathbf{i} \otimes t \mathbf{e}_1 \\ &= \exp jkz \exp \left[ \frac{jk}{2z} \left( \frac{a_f - 1}{a_f} \right) \mathbf{e}^2 \right] \mathbf{F}^{-1} \mathbf{F}[u_{i1} \mathbf{i}] \mathbf{F}[t \mathbf{e}_1] \\ &= \exp jkz \exp \left[ \frac{jk}{2z} \left( \frac{a_f - 1}{a_f} \right) \mathbf{e}^2 \right] \mathbf{F}^{-1} \mathbf{F}[u_{i1} \mathbf{i}] T \mathbf{f} \\ &= \exp jkz \exp \left[ \frac{jk}{2z} \left( \frac{a_f - 1}{a_f} \right) \mathbf{e}^2 \right] \mathbf{F}^{-1} \left( \mathbf{F} \left\{ \frac{u_i \mathbf{i}}{a_f} \exp \left[ \frac{jk}{2z} (1 - a_f \mathbf{i}^2) \right] \right\} T \mathbf{f} \right) \end{aligned} \quad (4.17)$$

Frequency components of  $\mathbf{f}$  is equal to the inverse of spatial coordinates. Then, setting  $a_f = 1$  in Eq.4.17, Eq.4.7 is obtained. Effect of random phase fluctuations is seen in Eq.4.18 adding a turbulent exponential to Eq.4.17.

$$u_e \mathbf{e}, z = \exp jkz \exp \left[ \frac{jk}{2z} \left( \frac{a_f - 1}{a_f} \right) \mathbf{e}^2 \right] \overbrace{\exp[\theta \mathbf{e}]}^{\text{random phase fluctuations}} \mathbf{F}^{-1} \left\{ \mathbf{F} \left[ \frac{u_i \mathbf{i}}{a_f} \exp \left[ \frac{jk}{2a} (1 - a_f) \mathbf{i}^2 \right] \right] T \mathbf{f} \right\} \quad (4.18)$$

Using convolution integral, Eq.4.18 can be calculated and below equations can be acquired.

$$u_{i2} \mathbf{i} = u_i \mathbf{i} \exp \left[ \frac{jk}{2z} (1 - a_f) \mathbf{i}^2 \right] \quad (4.19)$$

$$t \mathbf{e} - \mathbf{i} = \exp \left[ \frac{jk}{2z} a_f \left( \frac{\mathbf{e}}{a_f} - \mathbf{i} \right)^2 \right] = \exp \left[ \frac{jk}{2za_f} \mathbf{e} - a_f \mathbf{i}^2 \right] \quad (4.20)$$

Finally, received field expression turns into the form in Eq.4.21 independent of Fourier transform

$$\begin{aligned} u_e \mathbf{e}, z &= \frac{-jk \exp jkz}{2\pi z} \exp \left[ \frac{jk}{2z} \left( \frac{a_f - 1}{a_f} \right) \mathbf{e}^2 \right] \exp[\theta \mathbf{e}] u_{i2} \mathbf{i} \otimes t \mathbf{i} \\ &= \frac{-jk \exp jkz}{2\pi z} \exp \left[ \frac{jk}{2z} \left( \frac{a_f - 1}{a_f} \right) \mathbf{e}^2 \right] \exp[\theta \mathbf{e}] \int_{-\infty}^{\infty} \int_{-\infty}^{\infty} d^2 \mathbf{i} u_{i2} \mathbf{i} \exp \left[ \frac{jk}{2za_f} \mathbf{e} - a_f \mathbf{i}^2 \right] \end{aligned} \quad (4.21)$$

Received field expression is taken into account to calculate the received intensity.

$$\langle I(\mathbf{e}, z) \rangle = \langle u_e(\mathbf{e}, z) u_e^*(\mathbf{e}, z) \rangle \quad (4.22)$$

Using above equation, average intensity is derived as

$$\begin{aligned} \langle I_{e_x, e_y, z} \rangle &= \left( \frac{k}{2\pi z} \right)^2 \exp \left[ \frac{jke^2}{z} \left( \frac{a_f - 1}{a_f} \right) \right] \int_{-\infty}^{\infty} \int_{-\infty}^{\infty} \int_{-\infty}^{\infty} \int_{-\infty}^{\infty} d i_{1x} d i_{1y} d i_{2x} d i_{2y} u_i i_{1x}, i_{1y} u_i^* i_{2x}, i_{2y} \exp \left[ \frac{jk}{z} \left( \frac{e - a_f i}{a_f} \right) \right] \\ &\quad \left\langle \exp \left[ \theta i_{1x}, i_{1y} + \theta^* i_{2x}, i_{2y} \right] \right\rangle \end{aligned} \quad (4.23)$$

$\exp[\theta(\mathbf{e}, \mathbf{i})]$  term reduces to  $\exp[\theta(\mathbf{i})]$ , since there is no change on receiver plane coordinates. Wave structure function is defined as  $\theta \mathbf{e}_1, \mathbf{i}_1 + \theta^* \mathbf{e}_2, \mathbf{i}_2$  and in Cartesian coordinates it is written as

$$\left\langle \exp\left[\theta i_{1x}, i_{1y} + \theta^* i_{2x}, i_{2y}\right] \right\rangle = \exp\left[-\frac{|\mathbf{i}_1 - \mathbf{i}_2|^2}{\rho_e^2}\right] = \exp\left[-\frac{i_{1x}^2 + i_{2x}^2 + i_{1y}^2 + i_{2y}^2 - 2i_{1x}i_{2x} - 2i_{1y}i_{2y}}{\rho_e^2}\right] \quad (4.24)$$

where  $\rho_e$  refers to spatial coherence length. Coherence length has a formula as  $\rho_e = 0.545C_n^2 k^2 z^{-3/5}$  where  $C_n^2$  determines the turbulence level and it is very well known as structure constant. At the transmitter in such a communication system, truncated Bessel like beams are defined as

$$u_{i20} \mathbf{i} = M_c J_0 \alpha i \exp(-jn\psi) \exp\left[\frac{jk}{2z} (1 - a_f \mathbf{i}^2)\right] \quad (4.25)$$

Substituting  $u_{i20} \mathbf{i}$  into Eq.3.40 instead of  $u_{i2} \mathbf{i}$ , truncated Bessel beam expression over the receiver plane is analytically derived as

$$\begin{aligned} u_e \mathbf{e}, z &= \frac{-jk \exp jkz}{2\pi z} \exp\left[\frac{jk}{2z} \left(\frac{a_f - 1}{a_f}\right) \mathbf{e}^2\right] M_c J_0 \alpha i \exp(-jn\psi) \exp\left[\frac{jk}{2z} (1 - a_f \mathbf{i}^2)\right] \otimes t \mathbf{i} \\ &= \frac{-jk \exp jkz}{2\pi z} \exp\left[\frac{jk}{2z} \left(\frac{a_f - 1}{a_f}\right) \mathbf{e}^2\right] \int_{-\infty}^{\infty} \int_{-\infty}^{\infty} d^2 \mathbf{i} M_c J_0 \alpha i \exp(-jn\psi) \exp\left[\frac{jk}{2z} (1 - a_f \mathbf{i}^2)\right] \exp\left[\frac{jk}{2za_f} \mathbf{e} - a_f \mathbf{i}^2\right] \end{aligned} \quad (4.26)$$

## SECTION 5

### ADJUSTING 2-ASK & 4-ASK CONSTELLATION DIAGRAM

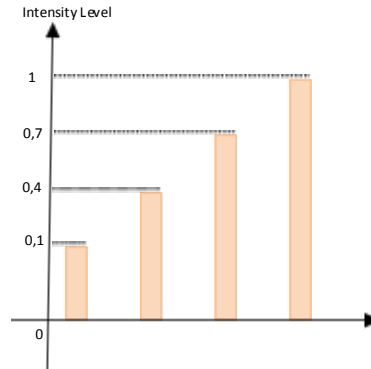
Modulation format characterizes transmitter and receiver systems. Simply, our simulation employed Amplitude-Shift Keying (ASK) for modulation which is also commonly called On-Off-Keying or Intensity Modulation (IM) where the laser is turned “On” to transmit a ”1” and turned “off” to demonstrate a “0”.

Composing this part, it has been utilized from Eyyuboğlu, H.T. article [50]. On the transmitter side, 21 mW optical power is shared between signal vectors equally and Truncated-Bessel Beam is generated according to following formula:

$$u_i(i_x, i_y) = m_n J_0(\alpha(i_x^2 + i_y^2)^{0.5})$$

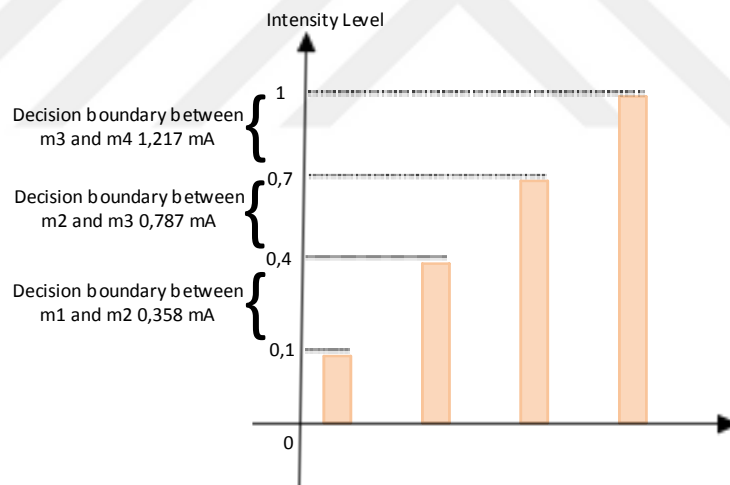
where  $(i_x, i_y)$  identify the truncation coordinates on the source plane,  $\alpha$  is width parameter which is set to 37,61 cm,  $m_n = \{m_1, m_2, m_3, m_4\} = \{0.1^2, 0.4^2, 0.7^2, 1\}$  that determine the signal vectors for 4-ASK modulation. On the other hand, during the 2-ASK modulation  $m_1, m_4$  are taken into account.

On the receiver side, receiver decision circuit needs to be trained against to the transmitted signals considering boundaries. During the 2-ASK modulation  $m_n = \{0.1^{0.5}, 1\}$  and during the 4-ASK modulation  $m_n = \{0.1^{0.5}, 0.4^{0.5}, 0.7^{0.5}, 1\}$  amplitude levels are identified. In the simulation, atmospheric effects parameters and propagation distance is kept constant then utilizing  $m_n = m_4 = 1$  maximum power transverse is done sending  $m_4$  constantly. On the source plane 4-ASK signal vector constellation diagram is illustrated on below figure 8 [50]:



**Figure 8:** 4-ASK Signal Vector Constellation on the Source Plane

4-ASK signal vector constellation diagram simulation results are evaluated precisely and symbol boundaries are assigned as following figure 9 [50] on the receiver side.



**Figure 9:** Decision Boundaries of 4-ASK Symbols on Receiver Side at  $C_n^2 = 10^{-13} m^{-2/3}$

It is well known that during IM the received photons integrated over the receiver aperture for conversion of the electrical current then we take into account just amplitude changes on receiver field therefore phase fluctuations are ignored. Also, as explained in section 3 Atmospheric Effects on FSO Links scintillation cause intensity fluctuations on the receiver side that is examined.



## SECTION 6

### MATLAB SIMULATION PARAMETER SETTINGS

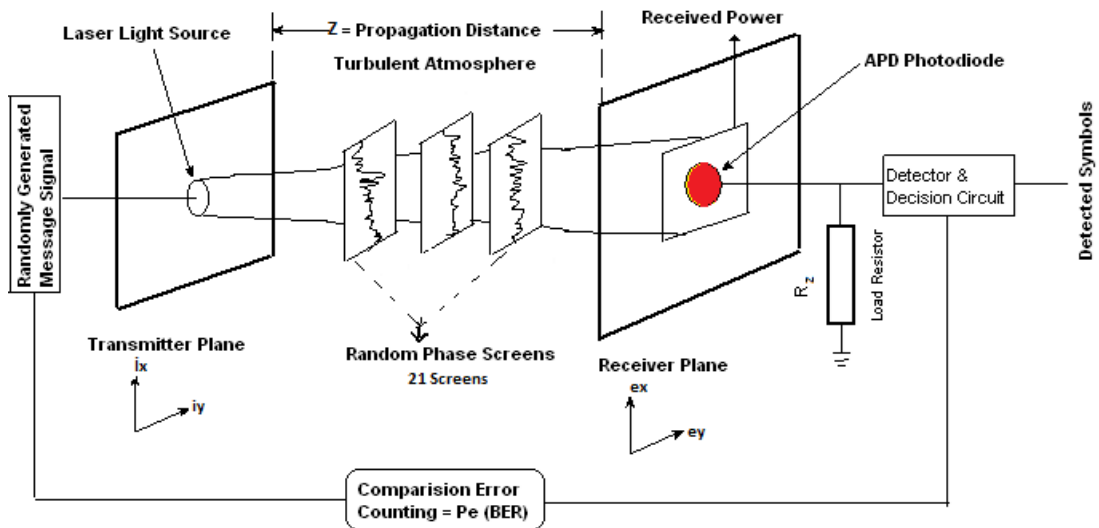
Simulation environment is simply illustrated at figure 10. Intensity modulation dependent communication link is established therefore message signals are indicated with  $m_1, m_2, m_3, m_4$  and  $10^5$  symbols are randomly generated by MATLAB randi function command. During the 2-ASK modulation  $m_1, m_4$  are taken into consideration. After the electrical messages have transferred into optical form, Bessel Beam is preferred on the laser-light-source because of its non-diffracting property [51, 52]. However, Bessel Beam contain an infinite amount of energy theoretically which is not physically realizable so zero-order Bessel Beam is truncated considering diffraction then zero order truncated Bessel beam is emitted from the 21 mW laser light source. Source plane dimensions are identified 40 cm X 40 cm corresponding to 512 x 512 grids [53, 54, 55] and grid intervals assigned to the constant d1 on the source plane.

Furthermore, the atmospheric turbulence beam propagation path is modelled by random phase screen planes and atmospheric turbulence conditions demonstrated with turbulence structure constant  $C_n^2$  which is arranged between  $10^{-15} m^{-2/3}$  and  $10^{-12} m^{-2/3}$ . According to the literature, 21 random phase screens are sufficient for 5 km FSO link length [56, 57, 58]. In this thesis, 21 intermediate random phase screens are kept for 3 km FSO line-of-sight horizontal propagation link distance that improves the reliability of consequences. During the beam propagation, grid intervals are growing and indicated with d2. Zero-order truncated Bessel beam intensity distribution is investigated throughout the atmospheric turbulence propagation.

On the receiver side, square aperture has been opened 6 cm x 6 cm and 140 cm x 140 cm for 2-ASK Bessel Beam Test and during the 4-ASK Bessel Beam Test opened square aperture is kept 140 cm x 140 cm. Then, photons are collected from receiver

plane which are converted into electrical current with help of photo-detector. Theoretically, as explained in section 7, shot and thermal noises are added to this current. Thermal noise parameters were arranged according to following values:

Boltzmann's constant  $C_B = 1.38 \times 10^{-23} m^2 kg s^{-2} K^{-1}$ , the temperature in Kelvin degrees  $T_K = 293K$ , the noise factor  $P_N = 2$ , the bandwidth  $B_W = 1 GHz$  the load resistor  $R_z = 50 \Omega$ . Then voltage is induced against the load resistor and decision circuit makes a decision regarding threshold which symbol is received. Justifying received symbol 500 realization carried out for each symbol. Determining decision thresholds, we take into consideration that the low level modulation was adjusted to % 10 of its high level to avoid nonlinear region of laser source [59]. Furthermore, operation wavelength is set to  $\lambda = 1.55 \mu m$ , beam wandering effects, beam spreading effects, beam jittering, wave-front distortions, angle-of-arrival fluctuations and lens attenuation are ignored as explained rationales in section 3.



**Figure 10:** Optical Link Simulation Model in Turbulent Atmosphere with Random Phase Screen Method

Note that while composing figure 10, re-printed with the permission from Ref. [60].

## SECTION 7

### SIGNAL TO NOISE RATIO DERIVATION

In this thesis Truncated-Bessel-Beam communication link has been established and propagated through the different simulated turbulent atmosphere conditions modeled by random phase screens. Corresponding to the different receiver aperture 2-ASK & 4-ASK modulation techniques are implemented and communication link performance is investigated regarding photo-detection performance. The investigation handled utilizing from BER which is generally performance evaluation parameter for digital communication systems. In the course of BER analyzing, it has been benefitted from SNR which is directly affected from incident optical power and noises [60]. Incident optical power collimated onto photo-detector that converts optical to electrical signals. During the conversion process, different types of noises are added to the received signal. When the rectangular shaped digital received signal is analyzed step by step, not only atmospheric effects but also photo-detector optical to electrical signal conversion process causes noise on the receiver side. In other words, the receiver current fluctuations derive from various noise mechanisms which compromise from photo-detector causing shot noise, load resistor causing thermal noise and atmosphere causing scintillation noise that are briefly explained in the below sections [60, 61].

#### 7.1 Shot Noise

Even if the incident optical power has a constant value on the photodiode, photons reach to the active area with different times, corresponding to the time difference between arrived photons, during the photons to electron conversion, current is

generated with dark current at random times, which lead to the statistical fluctuation on the received signal and shot noise mathematically is expressed:

$$\text{Shot noise : } \sigma_S^2 = 2q \left( A_{mf} R_{pr} \langle P_{in}(z) \rangle + I_{dk} \right) B_w \quad (7.1)$$

where  $I_{dk}$  is the dark current and  $B_w$  is the electrical bandwidth,  $A_{mf}$  avalanche photodiode multiplication factor,  $R_{pr}$  photodiode responsivity and  $q$  is the electron charge.

## 7.2 Thermal Noise

Thermal Noise or Johnson Noise is a fundamental noise source like as shot noise. Photodiode has a load resistor adds fluctuations to the current generated by the photodiode because of the thermal fluctuations and random motion of electrons in a conductor. It's calculated as below:

$$\text{Thermal noise : } \sigma_T^2 = 4C_B T_K B_w P_N / R_z \quad (7.2)$$

where  $C_B$  is the Boltzmann's constant,  $T_K$  is the temperature in Kelvin degrees,  $P_N$  is the noise factor,  $R_z$  is the load resistor.

## 7.3 Scintillation Noise

Optical communication link is propagating through the turbulent atmosphere having fluctuations in the refractive index which causes scintillation noise and calculated as below:

$$\text{Scintillation Noise : } \sigma_P^2 = A_{mf}^2 R_{pr}^2 \left[ \langle P_{in}^2(z) \rangle - \langle P_{in}(z) \rangle^2 \right] \quad (7.3)$$

The normalized received signal power on the photodiode described on below:

$$P_e = \langle I_{dk} \rangle^2 = A_{mf}^2 R_{pr}^2 \langle P_{in}(z) \rangle^2 \quad (7.4)$$

$$\begin{aligned}
\text{SNR} &= \frac{\text{signal power}}{\text{noise power}} = \frac{P_e}{\sigma_S^2 + \sigma_T^2 + \sigma_P^2} \\
&= \frac{A_{mf}^2 R_{pr}^2 \langle P_{in}^2(z) \rangle^2}{2q [A_{mf} R_{pr} \langle P_{in}(z) \rangle + I_{dk}] B_w + 4C_B T_K B_w P_N / R_z + A_{mf}^2 R_{pr}^2 [\langle P_{in}^2(z) \rangle - \langle P_{in}(z) \rangle^2]} \quad (7.5)
\end{aligned}$$

Analyzing of fluctuating current is to examine BER which is performance evaluation parameter for digital communication system. The rationales as explained in article [60], scintillation noise is dominant comparing to thermal and shot noise in other words,  $\sigma_P^2 \gg \sigma_S^2$  and  $\sigma_P^2 \gg \sigma_T^2$  in atmosphere. Receiver aperture size has the influence on SNR and BER performance [62]. The quality of received signal plays major role on threshold detection mechanism. It is clear that enlargement of receiver aperture not only collecting more received power but also fetching more scintillation noise.

Moreover, enlargement of the receiver aperture is described in terms of atmosphere coherence length, wavelength, propagation distance, structure constant and interrelations between them are defined in Ref. 63.

It is worth of saying that when intensity distribution is examined point by point, as move away from center of beam (on-axis), increasing scintillation noise effects are observed on the edges of spreading received beam. In this thesis, intensity distribution has been analyzed on the finite-sized receiver apertures in terms of field utilizing extended Huygens-Fresnel integral. During the symbol transmission receiver surface encounters several correlation patches concurrently aperture averaging is employing to handle and minimize high fluctuations on spatial axis for reducing power scintillation. While wavefront is consecutively hitting to same receiver surface, high fluctuations are diminishing with effect of aperture averaging in other words irradiance frequency spectrum is shifting lower frequencies by means of aperture averaging that simply suppresses the fastest fluctuations on the received signal [43]. Also, if correlation width larger than receiver aperture size, receiver

works as “point aperture” on the other hand, if receiver aperture size is larger than correlation width, irradiance fluctuations averaging operation will be performed over the finite size aperture to decrease scintillation effects [43].

Aperture averaging is used for in order to improve BER and SNR performance parameters in free space optical communication [64, 65, 66, 67, 68, 69]. Besides these theoretical studies, also experiments have been implemented on receiver aperture averaging method and measurements have been taken to prove the reliability of the aperture averaging approach [70, 71, 72]. Semi-analytical method has been used instead of complicated irradiance covariance function and power distribution of fluctuations is taken in Ref. [73] for different beams.

## SECTION 8

### EVALUATION of the SIMULATION RESULTS

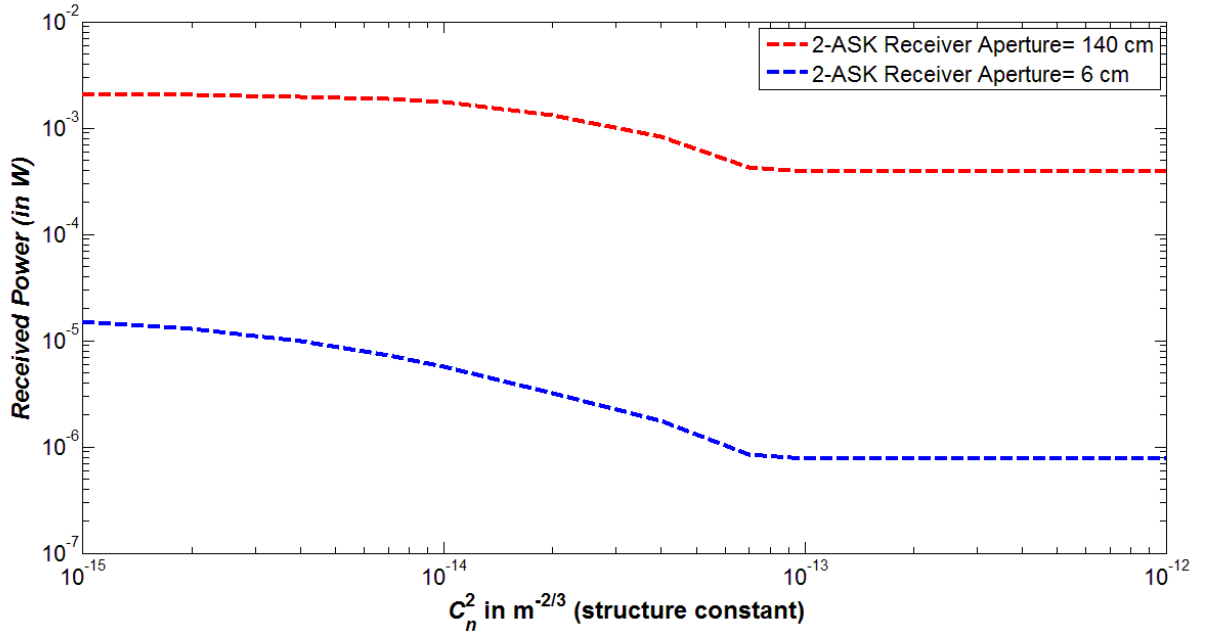
Literature reviewed for justify BER values, it has been encountered that in the simulation, estimated bit-error-rate should down to  $P_e = 10^{-4}$  in the digital communication systems [74].

In our simulation, analyzing MATLAB results figures have been drawn against the Received Power, SNR,  $P_e$  (digital communication performance parameters).

Additionally, in MATLAB simulation environment, atmospheric turbulence levels is varied by changing the structure constant which is range between  $10^{-15} m^{-2/3}$  and  $10^{-12} m^{-2/3}$  regarding atmospheric conditions [75]. As mathematically demonstrated in section 7, during the received power calculation thermal noise, shot noise and scintillation noise are ignored, but in course of SNR calculation all noises are taken into consideration.

In the Figure 11, Figure 12 and Figure 13, 2-ASK Modulated Truncated Bessel Beam is studied on two different receiver apertures against the varied structure constant.

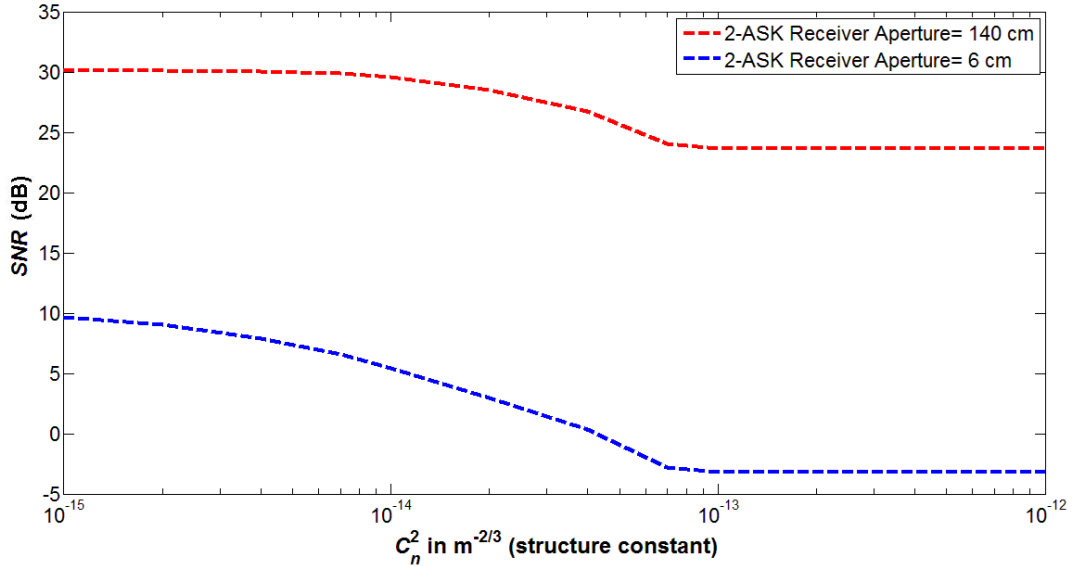
In Figure 14, Figure 15 and Figure 16, 2-ASK & 4-ASK Modulated Truncated Bessel Beam is analyzed against the varied atmospheric structure constant.



**Figure 11:** 2-ASK Modulated Truncated Bessel Beam versus the structure constant for different receiver aperture

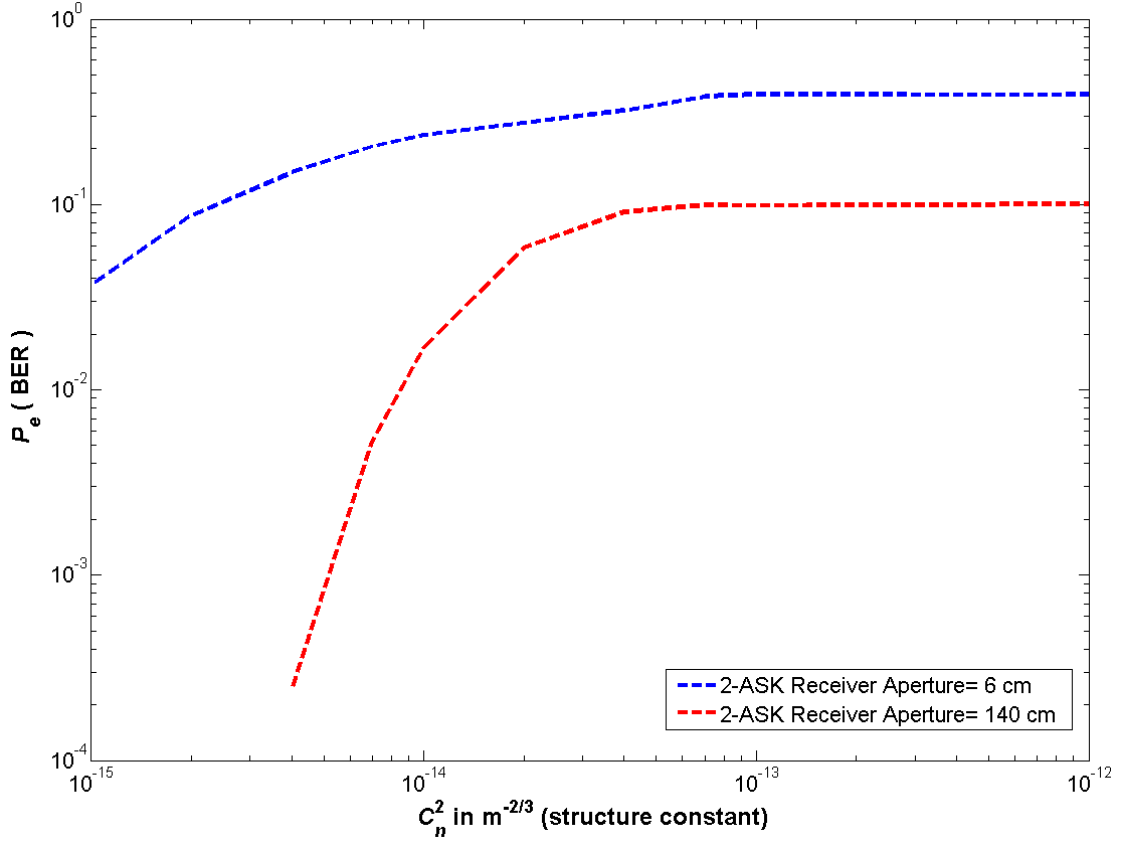
Figure 11 shows the Received Power Results on the receiver side. Using 140 cm receiver aperture more photons were collected therefore, it is observed that received power is directly related with opening receiver aperture. In spite of the changing atmospheric structure constant, approximately 100 times received power gap is kept and we have investigated that during the propagation we have sharply fall on received power about  $C_n^2 = 10^{-13} m^{-2/3}$  then we have encountered with constant received power between  $C_n^2 = 10^{-13} m^{-2/3}$  and  $C_n^2 = 10^{-12} m^{-2/3}$ .





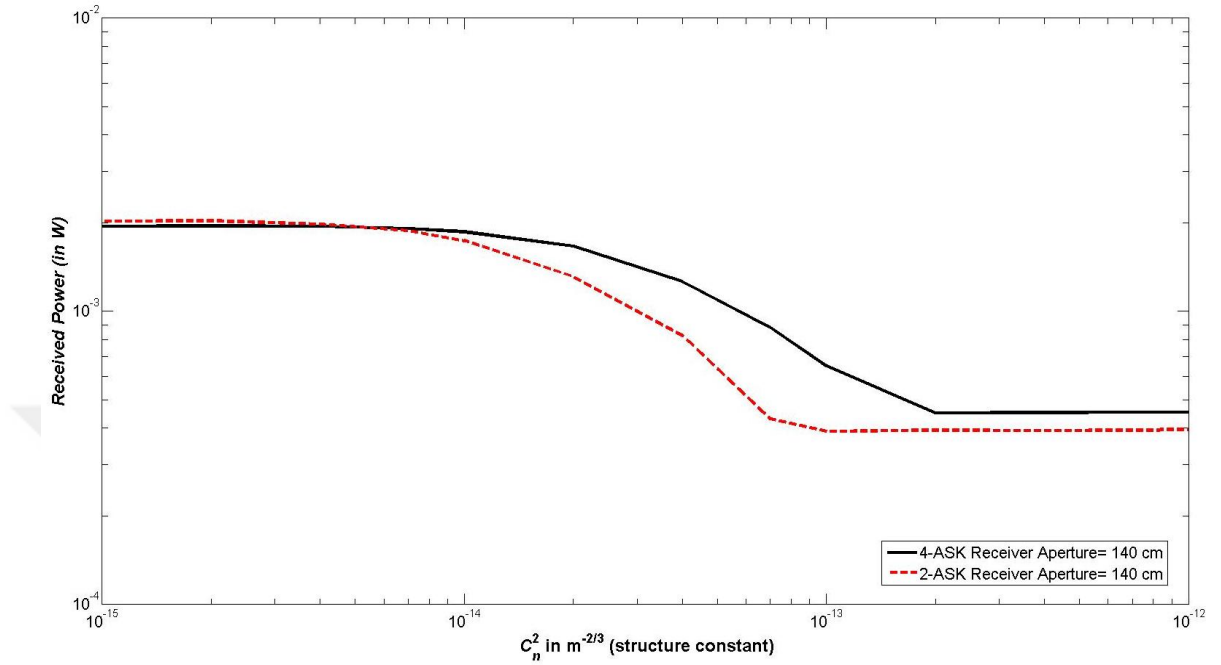
**Figure 12:** SNR behavior of the 2-ASK Modulated Truncated-Bessel-Beam versus to structure constant for different receiver aperture

In Figure 12, SNR variations are shown on the receiver side in terms of dB respect to changing structure constant. SNR and received power have interrelationship between each other which can be simply explained that received power indicates the numerator of the SNR without noises thus Figure 11 and Figure 12 have a similarity. As mentioned in Figure 11 explanation, almost 20 dB difference is observed at the  $C_n^2 = 10^{-15} m^{-2/3}$  but, increasing gap is observed throughout the varied structure constant so 6 cm receiver aperture received power is affected from noises more than 140 cm. As a result of increasing SNR gap,  $C_n^2 = 10^{-12} m^{-2/3}$ , nearly 30 dB SNR difference is sighted between each other.



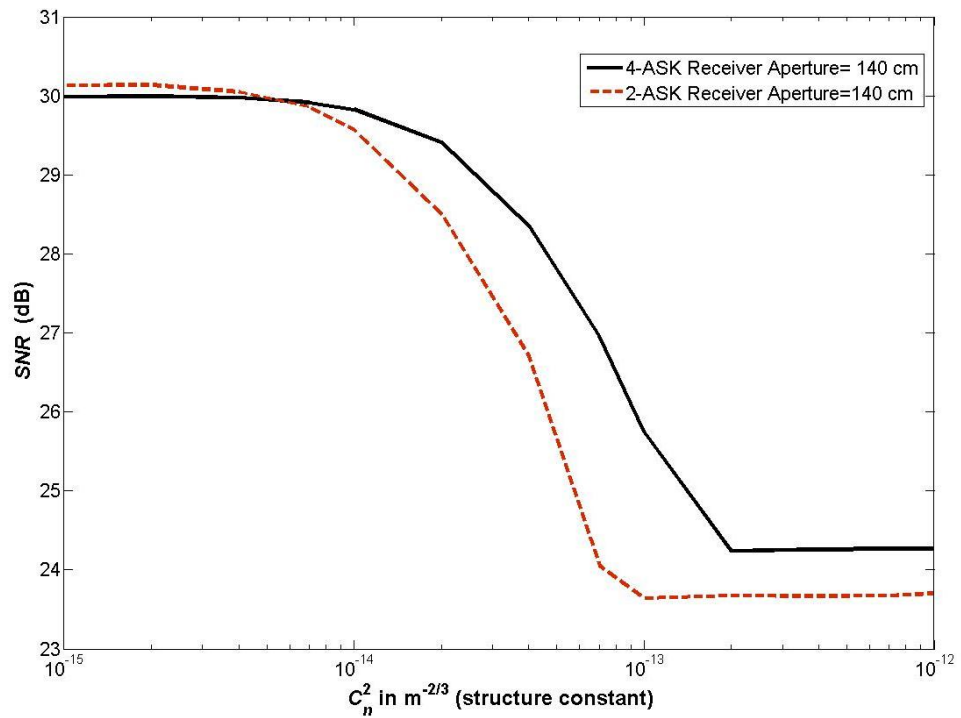
**Figure 13:**  $P_e$  (BER) behavior of the 2-ASK Modulated Truncated-Bessel-Beam versus to structure constant for different receiver aperture

Figure 13 demonstrates the probability of error performance against the varied structure constant. It is clear that BER is directly related with receiver aperture and structure constant. In clear atmosphere best performance BER (lowest  $P_e$ ) is offered by 140 cm receiver aperture on the other hand the its causes a sharp drop about  $C_n^2 = 10^{-14} m^{-2/3}$ , so  $C_n^2$  has a more impact on the big receiver aperture. As we sighted from Fig. 11 and Fig. 12, Y-axis data is linearly keeping stability between  $C_n^2 = 10^{-13} m^{-2/3}$  and  $C_n^2 = 10^{-12} m^{-2/3}$ .



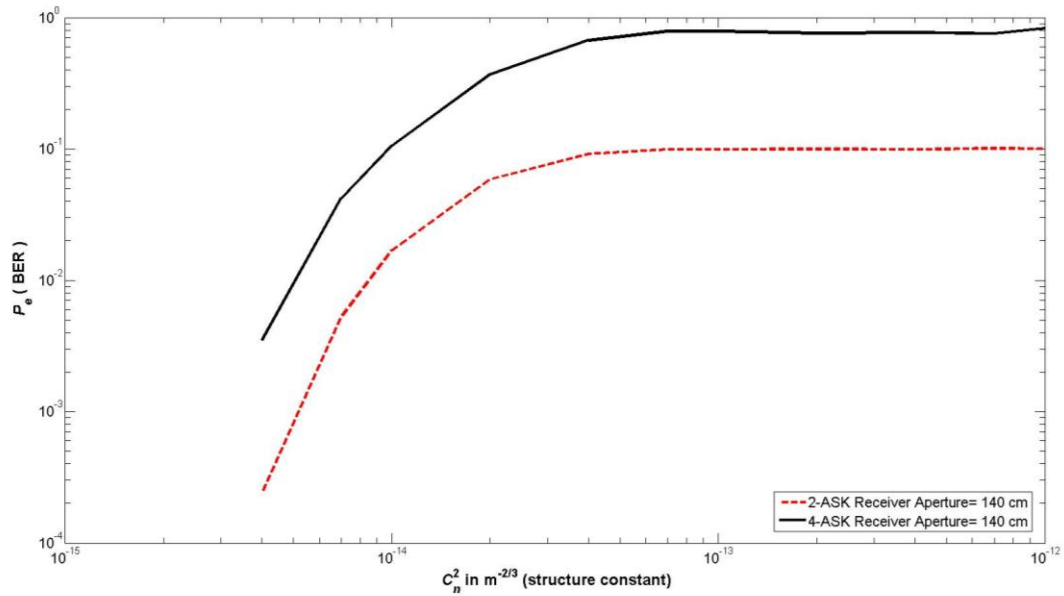
**Figure 14:** 2-ASK and 4-ASK Modulated Truncated Bessel Beam Received Powers versus the structure constant with identical receiver aperture

As it is explained section 5, there is no relation between modulation and received power which is affected from atmospheric effects and receiver aperture. It is clearly seen that using same receiver aperture approximately same powers are collected on the receiver. Also, it is worth to say that 2-ASK and 4-ASK modulated truncated Bessel beam are affected slightly different between  $C_n^2 = 10^{-14} m^{-2/3}$  and  $C_n^2 = 10^{-12} m^{-2/3}$ .



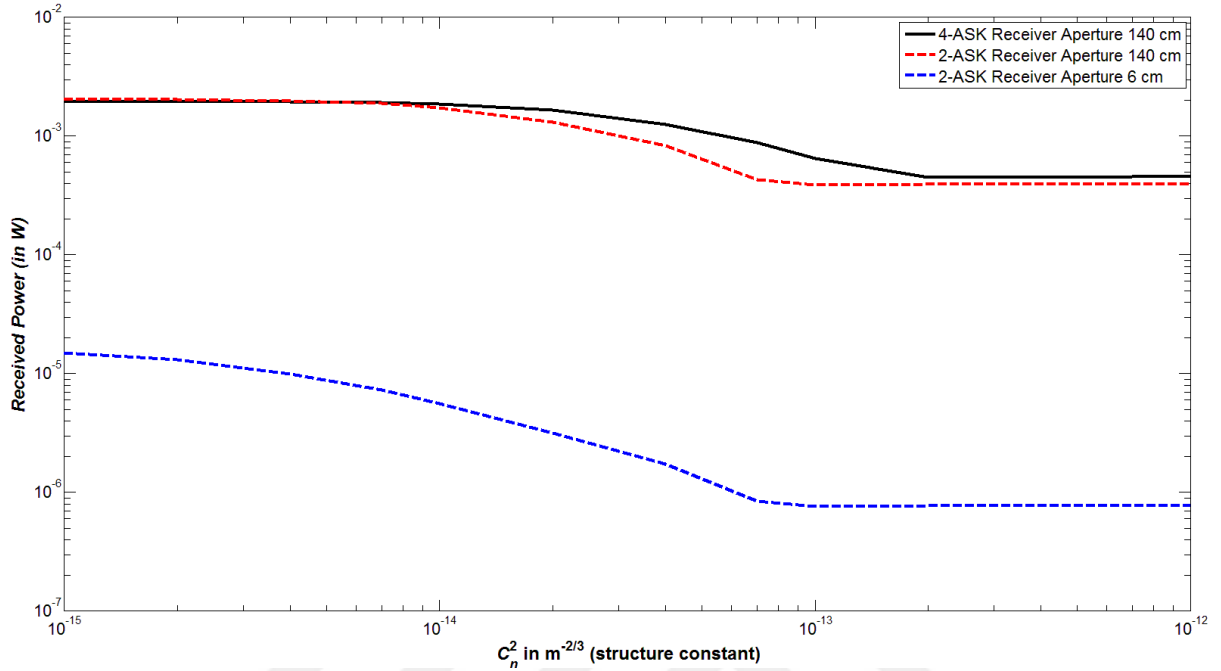
**Figure 15:** 2-ASK and 4-ASK Modulated Truncated Bessel Beam SNR against the structure constant with identical receiver aperture

As noise sources and rationales are explained in section 7, 2-ASK and 4-ASK modulated truncated Bessel beam are affected from atmospheric conditions which have nearly same sharp falling between  $C_n^2 = 10^{-14} m^{-2/3}$  and  $C_n^2 = 10^{-13} m^{-2/3}$  and while approaching medium and strong turbulent atmosphere condition, 2-ASK truncated Bessel beam is affected from noise more than 4-ASK.



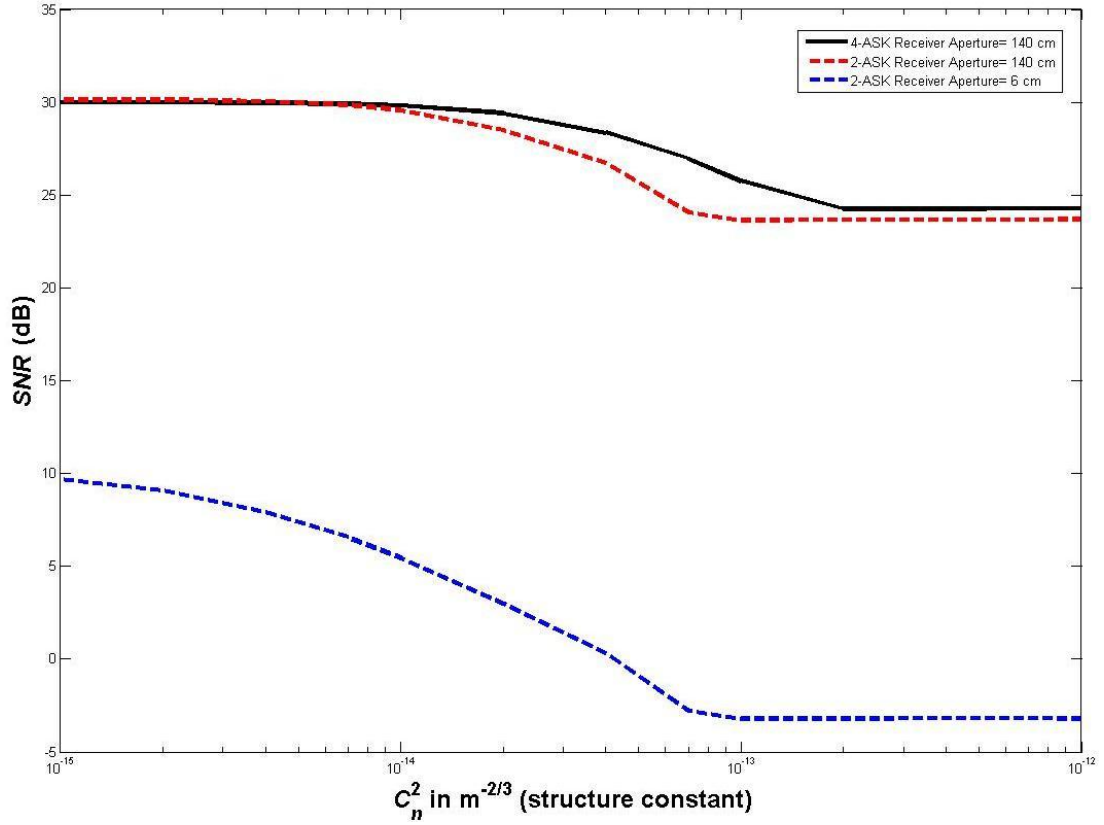
**Figure 16:** 2-ASK and 4-ASK Modulated Truncated Bessel Beam BER versus the structure constant with identical receiver aperture

In spite of the fact that 4-ASK truncated Bessel beam possess more SNR than the 2-ASK, 4-ASK has a poor BER or probability of error. In detail stated in section 5 minimum distance between symbols will influence on detection mechanism and 4-ASK symbol intervals are smaller than 2-ASK therefore, 4-ASK modulate truncated Bessel beam has worse BER than 2-ASK. It can be concluded that symbol distance plays major role on detection mechanism.



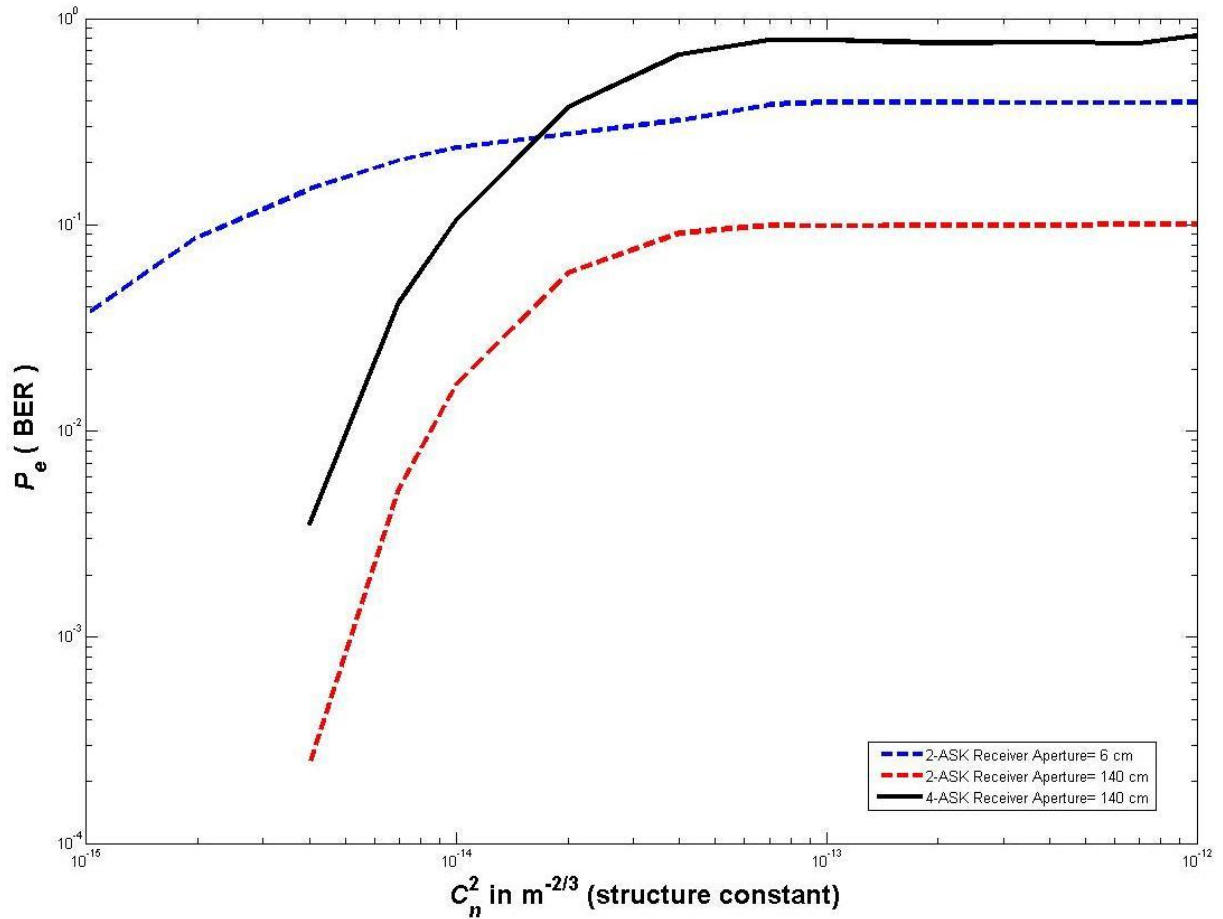
**Figure 17:** 2-ASK & 4-ASK Modulated Truncated Bessel Beam versus the structure constant for different receiver aperture

In addition to Fig.11, we have worked on 4-ASK modulated truncated Bessel beam to understand the structure constant effects on the modulation, then it is further examined the received power variations with respect to the varied  $C_n^2$ . Herewith, it can be said that 4-ASK modulated truncated Bessel beam received power is affected from scintillation less than 2-ASK between  $C_n^2 = 10^{-14} m^{-2/3}$  and  $C_n^2 = 10^{-12} m^{-2/3}$ .



**Figure 18:** 2-ASK & 4-ASK Modulated Truncated-Bessel-Beam SNR behaviors versus to structure constant for different receiver aperture

Regarding different receiver aperture 2-ASK & 4-ASK modulated truncated Bessel beam signal-to-noise ratio results are plotted towards to varied  $C_n^2$  for evaluating noises. In addition to Fig. 12, we can say that 4-ASK modulated truncated Bessel beam offers better signal performance than the others between  $C_n^2 = 10^{-14} m^{-2/3}$  and  $C_n^2 = 10^{-12} m^{-2/3}$ .



**Figure 19:** 2-ASK & 4-ASK Modulated Truncated-Bessel-Beam  $P_e$  (BER) behaviors versus to structure constant for different receiver aperture

Finally, figure 16 is drawn to assess structure constant impacts on 2-ASK & 4-ASK modulation and to explore the receiver aperture distinctive role on the BER performance. It can be clearly seen in Fig. 16 that even though 4-ASK modulated truncated Bessel beam possess the 140 cm receiver aperture, the worst BER performance is offered by 4-ASK modulated beam.



## SECTION 9

### CONCLUSION

In this thesis, 4-ASK & 2-ASK modulated truncated Bessel Beam are tested under different weak turbulent atmosphere conditions which are modeled by random phase screen method and constructed by MATLAB simulation environment. MATLAB run results are obtained in terms of received power, SNR and BER to compare the communication performance parameters. At the transmitter side, symbol array is generated and modulated in the form of 4-ASK & 2-ASK. Then these symbols are load over truncated Bessel beam and propagated through the weak turbulent atmosphere utilizing random phase screen method. At the receiver side, received field intensity is calculated with help of Huygens-Fresnel Integral over the receiver aperture plane then integral result is multiplied by its conjugate to calculate the received power on the receiver aperture. As explained in section 7, regarding literature shot noise, thermal noise and scintillation noise are modeled and generated then added to the received power to derive denominator of the SNR. Moreover, in course of MATLAB simulation atmospheric attenuation parameters are taken into consideration which are consisting of the absorption and scattering. Also, scintillation is regarded but beam wandering, beam spreading, beam jittering, wave-front distortions and angle-of-arrival fluctuations are ignored because of Rytov second-order approximation perturbations as explained in section 3. Under the above conditions finally, counting error symbols transmitted symbol array is compared with received symbol array to reach the BER. Consequently, analyzing receiver aperture effect 2-ASK & 4-ASK modulated truncated Bessel beam are examined against the different structure constant, between  $C_n^2 = 10^{-15} m^{-2/3}$  and  $C_n^2 = 10^{-12} m^{-2/3}$ , considering shot noise, thermal noise, scintillation noise. During the 2-ASK & 4-ASK truncated Bessel beam test versus the different structure constant, it is observed that big receiver aperture bring benefits in terms of received power and SNR but

BER performance is not only dependent on receiver aperture but also related with modulation and symbol constellation correspondingly, 4-ASK modulated truncated Bessel beam offered the worst BER performance in spite of 140 cm receiver aperture. Additionally, it is investigated that 4-ASK & 2-ASK truncated Bessel beams are affected in different way from various atmospheric conditions. The different influence is observed between  $C_n^2 = 10^{-14} m^{-2/3}$  and  $C_n^2 = 10^{-13} m^{-2/3}$  approximately.

On the other hand, to comprehend the working principle of FSO communication system, FSO architecture is researched from literature then practically FSO transmitter and receiver systems are designed for laboratory tests.

Consequently, truncated Bessel beam propagating turbulent atmosphere, 2-ASK & 4-ASK modulation effects and receiver aperture contribution are evaluated examining received power, SNR, BER performance parameters with respect to various structure.

## REFERENCES

1. **Majumdar, A.K.**, (2008), "*Free-space laser communication performance in the atmospheric channel*", in *Free-Space Laser Communication: Principles and Advances*, ed. by A.K. Majumdar, J. C. Ricklin. New York: Springer.
2. **Kartalopoulos, S.V.**, (2011), "*FREE SPACE OPTICAL NETWORKS FOR ULTRA-BROAD BAND SERVICES*", Editors: R. Abhari, M. El - Hawary O. P., Malik ,J. Anderson, B - M. Haemmerli, S. Nahavandi, G. W. Arnold, M. Lanzerotti, T. Samad, F. Canavero, D. Jacobson, G. Zobrist, Hanzo L. New Jersey & Canada: John Wiley & Sons, Inc., Hoboken.
3. **Davis, C.C., Smolyaninov, I.I.** (2002). "*Effect of atmospheric turbulence on bit-error rate in an on-off-keyed optical wireless system*". In *Free-Space Laser. Proc. SPIE 4489, Free-Space Laser Communication and Laser Imaging*, doi:10.1117/12.453236.
4. **Mahdieh M. H. and Pournoury M.**, (2010), "*Atmospheric turbulence and numerical evaluation of bit error rate (BER) in free-space communication*", *Opt. Laser Technol.*, vol. 42, pp. 55-60.
5. **Rodrigues, G. K. Carneiro, V. G. A. et.al.** (2013), "*Evaluation of the strong turbulence impact over free-space optical links*", *Opt. Commun.*305, 42–47.
6. **Fleck J.A., Morris JR, Feit MD** (1976), "*Time-dependent propagation of high energy laser beams through the atmosphere*", *Applied Physics* 1976;10(2):129–60.
7. **Coles, W.A., Filice J.P., Frehlich RG** (1995). "*Yadlowsky M. Simulation of wave propagation in three-dimensional random media*", *Applied Optics* 1995;34(12):2089–101.
8. **Davis, C.A., Walters D.L.** (1994), "*Atmospheric inner-scale effects on normalized irradiance variance*". *Applied Optics* 1994;33(36):8406–11.

9. **Nelson D.H., Walters D.L., MacKerrow E.P., Schmitt MJ, Quick CR, Porph WM, et.al.** (2000), “*Wave optics simulation of atmospheric turbulence and reflective speckle effects in CO2 lidar*”, Applied Optics 2000; 39(12):1857–71.
  
10. **Belmonte A.** (2000), “*Feasibility study for the simulation of beam propagation: consideration of lidar performance*”, Applied Optics 2000; 39(30):5426–45.
  
11. **Cheng W, Haus J.H., Zhan Q.** (2009), “*Propagation of vector beams through a turbulent atmosphere,*” Optics Express 2009;17(20):17829–36.
  
12. **Gu Y, Gbur G.** (2010), “*Scintillation of Airy beam arrays in atmospheric turbulence*” Optics Letters 2010;35(20):3456–8.
  
13. **Xiao X, Voelz D.** (2012) “*Annular beam propagation through turbulence: wave optics study of intensity and scintillation properties*”, IEEE aerospace conference 2012:1–6.
  
14. **Liu X, Pu J.** (2011), “*Investigation on the scintillation reduction of elliptical vortex beams propagating in atmospheric turbulence.*” Optics Express 2011;19 (27):26444–50.
  
15. **Durnin J.,** (1987), “*Exact solutions for non-diffracting beams. I. The scalar theory*”, J. Opt. Soc. Am. A, vol. 4, no. 4, 651-654.
  
16. **Gori F., Guattari G., Padovani C.,** (1987), “*Bessel-Gauss Beams*”, Opt. Commun., vol. 64, no. 6, pp. 491-495.
  
17. **Herman R. M. and Wiggins T. A.** (2000), “*Bessel-like beams modulated by arbitrary radial functions,*” J. Opt. Soc. Am. A 17, 1021–1032.
  
18. **Liu C., Chen S., Li X. Y., Xian H,** (2014) “*Performance evaluation of adaptive optics for atmospheric coherent laser communications*” Opt. Express. 22, 15554-63.

19. **Wang Z., Zhong W. –D., Fu S., Lin C., (2009)**, “*Performance Comparison of Different Modulation Formats Over Free-Space Optical (FSO) Turbulence Links With Space Diversity Reception Technique*”, IEEE Photon. J., vol. 1, no. 6, 276-285.
20. **Fried D.L.** (1967), “*Aperture Averaging of Scintillation*”, Journal of the Optical Society of America 1967;57(2):169–75.
21. **Lutomirski R.F., Yura H.T.**, (1969), “*Aperture-averaging factor of a fluctuating light signal*”, Journal of the Optical Society of America 1969;59(9):1247–8.
22. **Churside J.H.**, (1991) “*Aperture averaging of optical scintillations in the turbulent atmosphere*”, Applied Optics 1991;30(15):1982–94.
23. **Majumdar, A. K.** (2015), “*Modulation, Detection, and Coding for Free-space Optical (FSO) Communications*,” Advanced Free Space Optics (FSO), New York: Springer Series in Optical Sciences 186 pp: 69-70.
24. **Binh, Le N.** (2015). “*Modulation Formats and Optical Signal Generation*” in Advanced Digital Optical Communication Second Edition. Broken Sound Parkway NW: CRC Press pp: 3-9.
25. **Ravazi, B.** (2003). “*Generic Optical System*”, in Design of Integrated Circuit for Optical Communications. New York: McGraw-Hill, pp: 2-5.
26. **Fikar S., Bogenberger R., Arpad L.**, (2008), “*A 100GHz Bandwidth Matched Chip to PCB Transition Using Bond Wires for Broadband Matching*”, IEEE, BMW Group Research and Technology.
27. **Coonrod, J.** (2012), “*Selecting PCB Materials for High-Frequency Applications*”, Microwave Engineering Europe, pp. 18-20.
28. **Minoli, D.** (2003), “*Gigabit Ethernet/IEEE 802.3z*”, in Telecommunication Technology Handbook. Norwood, MA: Artech House Inc, pp:523-528.
29. Datasheet of LTC5100 3.3v, 3.2 Gbps VCSEL Driver (2003), Linear Technology Corporation, Milpitas, CA, Linear technology.

30. **Bespalko, R. D.**, (2007), “*Trans-impedance Amplifier Design using 0.18 um CMOS Technology*”, Queen's University, Kingston, Ontario, Canada.
31. **Wang, T., Erhman, B.**, (2005) “*Compensate Trans-impedance Amplifiers Intuitively*” Texas instruments, Application Report No: SBOA055A, March 1993– Revised March 2005.
32. **Ramus, X.** (2009) “*Trans-impedance Considerations for High-Speed Amplifiers*”, MAXIM, Application Report No: SBOA122A.
33. Datasheet of MAX3748 Compact 155Mbps to 4.25Gbps Limiting Amplifier (2011), MAXIM, 19-2717; Rev 6; 6/11
34. **Kartalopoulos, S.V.** (2011), “*1.6 The Atmosphere*”, in FREE SPACE OPTICAL NETWORKS FOR ULTRA-BROAD BAND SERVICES. Editors: R. Abhari, M. El - Hawary O. P., Malik ,J. Anderson, B - M. Haemmerli, S. Nahavandi, G. W. Arnold, M. Lanzerotti, T. Samad, F. Canavero, D. Jacobson, G. Zobrist, Hanzo L. New Jersey & Canada: John Wiley & Sons, Inc., Hoboken. pp: 9-10
35. **Tatarskii V.I (1971)**, “*The Effects of the Turbulent Atmosphere on Wave Propagation*”, National Technical Information Office, U.S. Department of Commerce, Springfield, VA 2216, pp: 218-258.
36. **Yu. N. Barabanenkov, Yu. A. Kravtsov, S.M. Rytov and V.I. Tatarskii**, (1960) “*Status of the Theory of Propagation of Waves in Randomly Inhomogeneous Medium,*” Soviet Phsics- Uspekhi, 13, No.5, pp: 551-580.
37. **Andrews, L. C. Phillips, R. L.** (2005). “*Chapter 6 Second-Order Statistics: Weak Fluctuation Theory*” in Laser Beam Propagation through Random Media Second Edition. USA Washington: SPIE—The International Society for Optical Engineering, pp: 181-182.

38. **Pisareva V.V.** (1960) “*Limits of Applicability of the Rytov Method of Smooth Perturbations in the Problem of Radiation Propagation through a Medium Containing In-Homogeneities,*” *Soviet Physics-Acoustics*, 6, No. 1, pp: 81-86.
39. **Bouchet, O. Sizun, H. Boisrobert, C. Fornel, F. Favennec, P.N.** (2006), “*Free-Space Optics Propagation and Communication*” Editor: P.N. Favennec France: Hermes Science/Lavoisier, USA: ISTE Ltd.
40. **McKechnie S.T.** (2016) “*General Theory of Light Propagation and Imaging Through the Atmosphere*”. USA: Springer Series in Optical Sciences, pp: 44-46.
41. **Andrews, L. C. Phillips, R. L.** (2005). “*Chapter 1.4 Atmospheric Effects*” in *Laser Beam Propagation through Random Media SECOND EDITION*. USA Washington: SPIE—The International Society for Optical Engineering, pp: 12-13.
42. **Blaunstein N., Arnon S., Zilberman A., Kopeika N.,** (2009), “*Applied Aspects of Optical Communication and Lidar*”, CRC Press, New York.
43. **Andrews, L.C. and Phillips R.L.** (2005) “*Laser Beam Propagation Through Random Media*”. SPIE Optical Engineering Press Bellingham, WA.
44. **Qian X., Zhu W., and Rao R.** (2009) “*Numerical investigation on propagation effects of pseudo-partially coherent Gaussian Schell-model beams in atmospheric turbulence,*” *Opt. Express* 17, pp: 3782-3791.
45. **Cheng W., J.H. Haus, and Q. Zhan,** (2009) “*Propagation of vector vortex beams through a turbulent atmosphere,*” *Optical Express* 17, 17829-17836.
46. **Liu X. and J. Pu,** (2011) “*Investigation on the scintillation reduction of elliptical vortex beams propagating in atmospheric turbulence,*” *Optical Express* 19, 26444-26450.

47. **Eyyuboğlu H.T.**, (2013) “*Estimation of aperture averaged scintillations in weak turbulence regime for annular, sinusoidal and hyperbolic Gaussian beams using random phase screen,*” *Optical Laser Technology*. 52, pp: 96-102.
48. **Bayraktar M.** (2015), “*Comparison of probability of error performance for truncated Bessel and Bessel Gauss Beams*” pp: 24-29.
49. **Schmidt J.D.**, (2010), “*Numerical Simulation of Optical Wave Propagation with Examples in MATLAB*”, SPIE, Washington, USA.
50. **Eyyuboğlu H. T.** (2016) “*Correction of amplitude distortions for truncated Bessel beam and SER estimation for 4-ASK*”, *Journal of Modern Optics*, DOI: 10.1080/09500340.1154197.
51. **Durnin J.** (1987) “*Exact solutions for non-diffracting beams, I. The Scalar Theory*”, *J. Opt Soc Am A* 1987; 4: 651–4.
52. **Borghi R, Santarsiero M, Gori F.** (1997), “*Axial intensity of apertured Bessel beams,*” *J Opt Soc Am A* 1997;14: 23–6.
53. **Johnston R.A., Lane R.G.**, (2000), “*Modeling scintillation from an aperiodic Kolmogorov phase screen,*” *Applied Optics* 2000; 39(26): 4761–9.
54. **Belmonte A.** (2000) “*Feasibility study for the simulation of beam propagation: consideration of lidar performance,*” *Applied Optics* 2000; 39(30): 5426–45.
55. **Schmidt J.D.**, (2010), “*Numerical Simulation of Optical Wave Propagation with examples in MATLAB,*” Washington: SPIE Press.
56. **Andrews, L. C. Phillips, R. L.** (2005). “*Section 15 Propagation Through Random Phase Screens*” in *Laser Beam Propagation through Random Media* Second Edition. USA Washington: SPIE—The International Society for Optical Engineering pp: 647-663
57. **Macaskill C., Ewart T.E.**, (1984), “*Computer simulation of two-dimensional random wave propagation*”, *IMA Journal of Applied Mathematics* 1984;33(1):pp: 1–15.



58. **Coles Wm. A., Filice J.P., Frehlich R.G, Yadlowsky M.,** (1995), “*Simulation of wave propagation in three-dimensional random media*”, Applied Optics 1995;34(12):2089-2101
59. **Agrawal G. P.,** (2002), “*Fiber-Optic Communication Systems*” New York: JOHN WILEY & SONS, INC., PUBLICATION ISBN: 0-471-22114-7.
60. **Eyyuboğlu H. T. and Bayraktar M.,**(2015), “*SNR bounds of FSO links and its evaluation for selected beams*”, J. Modern Opt. vol. 62, no. 16, pp. 1316-1322.
61. **Agrawal G.P.,** (2007) “*Optical Communication Systems*”, Institute of Optics, Rochester.
62. **Kaushal H., Kaddoum G.** (2015) “*Free Space Optical Communication: Challenges and Mitigation Techniques,*” India-122017, arXiv: 1506.04836v1.
63. **M.A. Khalighi, N. Aitamer, N. Schwartz, S. Bourennane** (2009) “*Turbulence Mitigation by Aperture Averaging in Wireless Optical Systems*” , Marseille France, ISBN: 978-953-184-131-3.
64. **F. S. Vetelino, C. Young, L. C., Andrews, and J. Rekolons,** (2007) “*Aperture averaging effects on the probability density of irradiance fluctuations in moderate-to-strong turbulence,*” Applied Optics, vol. 46, no. 11, pp. 2099–2108.
65. **J. H. Churnside,** (1991) “*Aperture averaging of optical scintillations in the turbulent atmosphere,*” Applied Optics, vol. 30, no. 15, pp. 1982–1994.
66. **L. C. Andrews,** (1992) “*Aperture-averaging factor for optical scintillations of plane and spherical waves in the atmosphere,*” Journal of Optical Society of America (JOSA) A, vol. 9, no. 4, pp. 597–600.
67. **L. C. Andrews, R. L. Phillips, and C. Y. Hopen,** (2000) “*Aperture averaging of optical scintillations: power fluctuations and the temporal spectrum,*” Waves Random Media, vol. 10, pp. 53–70.
68. **F. S. Vetelino, C. Young, and L. C. Andrews,** (2007) “*Fade statistics and aperture averaging for Gaussian beam waves in moderate-to-strong turbulence,*” Applied Optics, vol. 46, no. 18, pp. 3780–3789.

69. **G. L. Bastin, L. C. Andrews, R. L. Phillips, R. A. Nelson, B. A. Ferrel, M. R. Borbathe, D. J. Galuse, P. G. Chine, W. G. Harrisa, J. A. Mar'ina, G. L. B. D. Wayne, and R. Pescatore,** (2005) "*Measurements of aperture averaging on bit-error-rate,*" Proceedings of SPIE, Atmospheric Optical Modeling, Measurement, and Simulation, vol. 5891, pp. 02-1 – 02-12.
70. **N. Perlot and D. Fritzsche,** (2004) "*Aperture-averaging, theory and measurements,*" Proceedings of SPIE, Free-Space Laser Communication Technologies XVI, vol. 5338, pp. 233-242.
71. **L. M. Wasiczko and C. C. Davis,** (2005) "*Aperture averaging of optical scintillations in the atmosphere: experimental results,*" Proceedings of SPIE, Atmospheric Propagation II, vol. 5793, pp. 197-208.
72. **J. Chen, Y. Ai,** (2010) "*Laser signal intensity and aperture averaging analysis in 16km free-space optical links*", IEEE, 978-1-4244-4964-4/10.
73. **H.T. Eyyubođlu,** (2014) "*Apertured averaged scintillation of fully and partially coherent Gaussian, annular Gaussian, flat topped and dark hollow beams*" Science Direct, Elsevier, Optics Communications 339 (2015) 141-147.
74. **Jeruchim M.C.,** (1984) "*Techniques for estimating the bit error rate in the simulation of digital communication systems,*" IEEE J. Sel. Areas Commun. 2, pp: 153-170.
75. **Grabner M., Kvivera V.,** (2012) "*Measurement of the Structure Constant of Refractivity at Optical Wavelengths Using a Scintillometer,* " RadioEngineering, VOL: 21, No: 1.

**APPENDICES A**  
**CURRICULUM VITAE**



**PERSONAL INFORMATION**

**Surname, Name:** Ađar, Tevfik

**Date and Place of Birth:** 17 September 1989, Ankara

**Marital Status:** Single

**Phone:** +90 541 288 23 62

**Email:** tevfikagar@gmail.com

**EDUCATION**

<b>Degree</b>	<b>Institution</b>	<b>Year of Graduation</b>
B.Sc.	Çankaya Univ., Electronic and Communication Engineering	2013
High School	Çankaya High School	2008

**WORK EXPERIENCE**

<b>Year</b>	<b>Place</b>	<b>Enrollment</b>
2014 - Present	FOTONİKS Askeri Elektronik ve Elektro-Optik A.Ş.	Avionic System Requirement Manager Design Engineer
2014 - Present	Lazersan Haberleşme	Co-Founder
2013 - Present	Lazersan Elektronik	Co-Founder

2012	TAI	Intern
2011	ASELSAN	Intern
2006-2012	Çetinkaya İletişim	Technician

## **FOREIN LANGUAGES**

Advanced English and Beginner Spanish

## **PROJECTS**

1. F-16 Head Up Display
2. Hurkus-B Head Up Display
3. Hurkus-B Control Panel
4. Visible Light Communication System, Project Number: 0082.TGSD.2014, Ministry of Science, Industry and Technology, 2014.
5. Free Space Optics Modem, Project Number: 0935.TGSD.2013, Ministry of Science, Industry and Technology, 2013.

## **CERTIFICATIONS**

1. PTC Windchill Product Lifecycle Management Quality Solutions
2. PTC Windchill Product Lifecycle Management FMEA & Prediction
3. PTC Windchill Product Lifecycle Management Heavy User
4. PTC Windchill Product Lifecycle Management Light User
5. IBM - Rational DOORS Requirement Management
6. Yeni İşler Yeni Fikirler Entrepreneurship
7. KOSGEB Entrepreneurship
8. C# Programming Language
9. Junior Alcatel Lucent

10. NLP Expert

### **HONOURS AND AWARDS**

1. “Yeni Fikirler Yeni İşler 2014“ competition 2<sup>st</sup> degree in category of Energy
2. “Yeni Fikirler Yeni İşler 2013“ competition 1<sup>st</sup> degree in category of Defence Industry
3. “Yeni Fikirler Yeni İşler 2013 “ competition 2<sup>st</sup> degree in category of Information Technology
4. Graduated High Honor Student in 2013 from Çankaya University

### **HOBBIES**

Travelling, Books, Cycling, Ride a bicycle